environmental microbiology

Environmental Microbiology (2021) **23**(7), 3435–3459 doi:10.1111/1462-2920.15166

Transcriptomic analysis of polyaromatic hydrocarbon degradation by the halophilic fungus *Aspergillus sydowii* at hypersaline conditions

Heidy Peidro-Guzmán,[1] Yordanis Pérez-Llano,[1] Deborah González-Abradelo,[1] Maikel Gilberto Fernández-López,[1] Sonia Dávila-Ramos,[1] Elisabet Aranda,[2] Darío Rafael Olicón Hernández,[2] Angélica Ortega García,[1] Verónica Lira-Ruan,[1] Oscar Ramírez Pliego,[1] María Angélica Santana,[1] Denhi Schnabel,[3] Irina Jiménez-Gómez,[1] Rosa R. Mouriño-Pérez,[4] Elva T. Aréchiga-Carvajal,[5] María del Rayo Sánchez-Carbente,[6] Jorge Luis Folch-Mallol,[6] Ayixon Sánchez-Reyes,[7] Vinoth Kumar Vaidyanathan,[8] Hubert Cabana,[9] Nina Gunde-Cimerman[10] and Ramón Alberto Batista-García [1*]

[1]*Centro de Investigación en Dinámica Celular, Instituto de Investigación en Ciencias Básicas y Aplicadas, Universidad Autónoma del Estado de Morelos, Cuernavaca, Morelos, Mexico.*

[2]*Instituto Universitario de Investigación del Agua, Universidad de Granada, Granada, Spain.*

[3]*Instituto de Biotecnología, Universidad Nacional Autónoma de México, Cuernavaca, Morelos, Mexico.*

[4]*Centro de Investigación Cientifica y Educación Superior de Ensenada, Ensenada, Baja California, Mexico.*

[5]*Facultad de Ciencias Biológicas, Unidad de Manipulación Genética, Universidad Autónoma de Nuevo León, Monterrey, Nuevo León, Mexico.*

[6]*Centro de Investigación en Biotecnología, Universidad Autónoma del Estado de Morelos, Cuernavaca, Morelos, Mexico.*

[7]*Cátedras Conacyt – Instituto de Biotecnología, Universidad Nacional Autónoma de México, Cuernavaca, Morelos, Mexico.*

[8]*SRM Institute of Science and Technology, Kattankulathur, Tamil Nadu, India.*

[9]*Faculté de Genié, Université de Sherbrooke, Sherbrooke, Quebec, Canada.*

[10]*Departament of Biology, Biotechnical Faculty, University of Ljubljana, Ljubljana, Slovenia.*

Received 7 May, 2020; revised 11 July, 2020; accepted 12 July, 2020. *For correspondence. E-mail rabg@uaem.mx, rbatista25@yahoo.com; Tel. (+52) 777 3297020; Fax +527773297020. Heidy Peidro-Guzmán, Yordanis Pérez-Llano and Deborah González-Abradelo contributed equally to this work.

Summary

Polycyclic aromatic hydrocarbons (PAHs) are among the most persistent xenobiotic compounds, with high toxicity effects. Mycoremediation with halophilic *Aspergillus sydowii* was used for their removal from a hypersaline medium (1 M NaCl). *A. sydowii* metabolized PAHs as sole carbon sources, resulting in the removal of up to 90% for both PAHs [benzo [*a*] pyrene (BaP) and phenanthrene (Phe)] after 10 days. Elimination of Phe and BaP was almost exclusively due to biotransformation and not adsorption by dead mycelium and did not correlate with the activity of lignin modifying enzymes (LME). Transcriptomes of *A. sydowii* grown on PAHs, or on glucose as control, both at hypersaline conditions, revealed 170 upregulated and 76 downregulated genes. Upregulated genes were related to starvation, cell wall remodelling, degradation and metabolism of xenobiotics, DNA/RNA metabolism, energy generation, signalling and general stress responses. Changes of LME expression levels were not detected, while the chloroperoxidase gene, possibly related to detoxification processes in fungi, was strongly upregulated. We propose that two parallel metabolic pathways (mitochondrial and cytosolic) are involved in degradation and detoxification of PAHs in *A. sydowii* resulting in intracellular oxidation of PAHs. To the best of our knowledge, this is the most comprehensive transcriptomic analysis on fungal degradation of PAHs.

Introduction

Polycyclic aromatic hydrocarbons (PAHs) constitute a heterogeneous group of persistent organic pollutants with two or more fused benzene rings (Haritash and Kaushik, 2009). These toxic, carcinogenic and mutagenic compounds are

generated during natural events like wildfires and volcanic eruptions, or due to anthropogenic activities such as the burning of fossil fuels, wood, garbage, municipal solid waste and oil spills (Haritash and Kaushik, 2009). They significantly contribute to the pollution of aquatic ecosystems and world's water resources (Liu *et al*., 2020). Mycoremediation has emerged as a promising and eco-friendly strategy to remove PAHs from environment (Aranda, 2016; Ali *et al*., 2019; Prenafeta-Boldú *et al*., 2019). It is based on the metabolic enzymatic transformation of PAHs by fungi into harmless substances (Ward *et al*., 2003; Aranda, 2016; Prenafeta-Boldú *et al*., 2019).

Although the removal of PAHs by filamentous fungi has been extensively investigated, the underlying molecular mechanisms remain poorly understood. High throughput RNA sequencing has not been widely used to examine the physiological changes during polyaromatic stress in filamentous fungi (Hernández-López *et al*., 2015; Gao *et al*., 2019; Loss *et al*., 2019). These studied demonstrated that genes involved in metabolism of xenobiotics and general stress responses were found upregulated during fungal growth on high-weight polyaromatic hydrocarbons. These also suggested that intracellular pathways play a greater role in PAH biodegradation by ascomycetes than was previously assumed (Hernández-López *et al*., 2015; Gao *et al*., 2019; Loss *et al*., 2019). Transcriptomics has also allowed the identification of new genes involved in the cellular response to PAHs (e.g. NF-κB-type transcriptional regulators) (Loss *et al*., 2019). Despite advances in the field, new studies using different omics approaches are needed for in depth understanding of the molecular and cellular mechanisms related to PAH biodepletion in ascomycetes.

Aquatic environments contaminated with PAHs might be saline or hypersaline as in the case of marine oil spills, oil extraction sites and wastewater from the petrochemical industry (McGenity, 2010). Salinity imposes an additional challenge to mycoremediation by preventing growth of non-adapted fungi. High NaCl concentrations affect protein structure and reduce the solvation layer of extracellular enzymes, hindering the biodegradation of xenobiotics. These adverse biophysical effects diminish the assimilation levels of PAHs in non-salt-adapted microorganisms (Kargi and Dinçer, 2000; McGenity, 2010; Oluwadara *et al*., 2017). Moreover, hypersaline conditions decrease the solubility of hydrocarbons, which is a crucial factor for their bioavailability. Oxygen is also less soluble in salty media (McGenity, 2010). This fact negatively influences the hydrocarbon biodegradation rate, as oxygen is a limiting reactant in hydrocarbon biodepletion mechanisms (McGenity, 2010). Few halophilic/halotolerant fungal strains have been identified as PAH degraders under salinity conditions (Lahav *et al*., 2002; Obuekwe *et al*., 2004; Hidayat *et al*., 2012; González-Abradelo *et al*., 2019), but little has been investigated about the mechanisms by which this degradation takes place.

Aspergillus sydowii EXF-12860 is a halophilic ascomycete fungus, with ligninolytic activity (Batista-García *et al*., 2014) and the ability to degrade PAHs and other xenobiotic compounds in hypersaline conditions (Batista-García *et al*., 2017; González-Abradelo *et al*., 2019). In this study we focused on the metabolic degradation of two PAHs – phenanthrene (Phe) and benzo [*a*] pyrene (BaP) – when present as sole carbon sources at hypersaline conditions (1 M NaCl) by the halophilic *A. sydowii* EXF-12860. Phe and BaP have been selected as model molecules, representing three- and five-ring PAHs with different physicochemical and toxicological properties (Bisht *et al*., 2015). We followed the metabolic mechanisms of PAHs degradation by analysing the transcriptomes of *A. sydowii* EXF-12860 growing with glucose or PAH as sole carbon source. Biochemical and toxicological studies were performed to determine the residual toxicity and thus to elucidate the potential of EXF-12860 for the bioremediation of hypersaline waters contaminated by PAHs.

Results

*Degradation of phenanthrene and benzo [*a*] pyrene by* A. sydowii

The removal of Phe and BaP from hypersaline (1 M NaCl) liquid media with PAHs as the sole carbon source, by *A. sydowii* had a similar profile for both polyaromatic substrates (Fig. 1A). During the first day of culture, the PAHs were mainly adsorbed onto the mycelium, reaching high levels of depletion (70% and 75% for BaP and Phe respectively), followed by desorption, releasing almost half of the adsorbed PAHs into the medium.

Degradation started after 2 days, resulting in the removal of up to ∼90% for both PAHs after 10 days of culture (Fig. 1A). Elimination of Phe and BaP by dead mycelium was very low (< 1%), even after 10 days of culture (data not shown), indicating that biotransformation – and not adsorption – was the main removal process. Within 10 days *A. sydowii* was able to degrade up to 71% of BaP and 73% of Phe under hypersaline conditions (Fig. 1A). These processes were accompanied by drastically decreased chemical oxygen demand (COD), from ∼97% after 12 h of mycotreatments to 99.8% after 10 days (Fig. 1B).

The degradation of PAHs has been correlated with a reduction in the medium pH, due to the release of 1-hydroxy-2-naphthoic acid, an early intermediate of Phe metabolism, as well as due to the release of phthalic acid or protocatechin acid, both produced during Phe degradation (Sun *et al*., 2020). For this reason we evaluated

changes in pH during the growth of *A. sydowii* in the presence of Phe and BaP (Fig. 1B). pH remained almost unchanged in non-inoculated media (~5.7–5.8) but dropped to ~4.8 after 4 days in cultures of *A. sydowii*, coinciding with the maximal PAH degradation and COD reduction. Afterwards the pH slowly increased and reached ~5.2 on day 10 (Fig. 1B), supporting the notion that acidic intermediates of the PAH degradation are later assimilated by the fungal mycelium.

Extracellular lignin modifying enzymes (LME), such as laccases, manganese peroxidases, unspecific peroxygenases (UPO) and esterases were measured in cultures of *A. sydowii*. These enzymes are potentially involved in PAH biotransformation in culture supernatant (Aranda, 2016; González-Abradelo *et al*., 2019), although total degradation of PAH by these enzymes has not been unequivocally determined in ascomycetes (Aranda, 2016; Aranda *et al*., 2017). As shown in Fig. 1C, laccase and manganese peroxidase activities peaked on the second day and slightly decreased thereafter, while esterase activity peaked on the fourth day. UPO activity was not detected.

We hypothesized that the greatest transcriptional changes take place during the active phase of PAH assimilation. Thus, we focused on PAHs degradation profiles to choose the appropriate time frame for transcriptomic analysis. The degradation of Phe began immediately (~7% in 12 h), whereas the degradation of the more complex BaP was observed after 1 day in culture (Fig. 2A). The rate of PAH conversion was exponential between 1 and 4 days (R^2 = 0.998, Spearman correlation coefficient). Therefore, the extraction of total RNA for transcriptome analysis was conducted after 3 days of culture (Fig. 2A), when *A. sydowii* reached the maximum degradation velocity.

As cytochromes (CYCs) [e.g. cytochromes P450 (CYPs)] are widely recognized for their involvement in PAH biotransformation in ascomycetes (Aranda, 2016; Loss *et al*., 2019), the role of CYCs during the PAH assimilation in *A. sydowii* was investigated. NADPH-CYC *c* reductase activity was determined after three days of mycotreatment in the presence of the CYC inhibitor piperonyl butoxide (PPB) (Haroune *et al*., 2016), resulting in partial inhibition of CYCs by adding 1.0 mM and 10 mM PPB (Fig. 2B). Both concentrations of the CYC inhibitor were sufficient to reduce the Phe and BaP

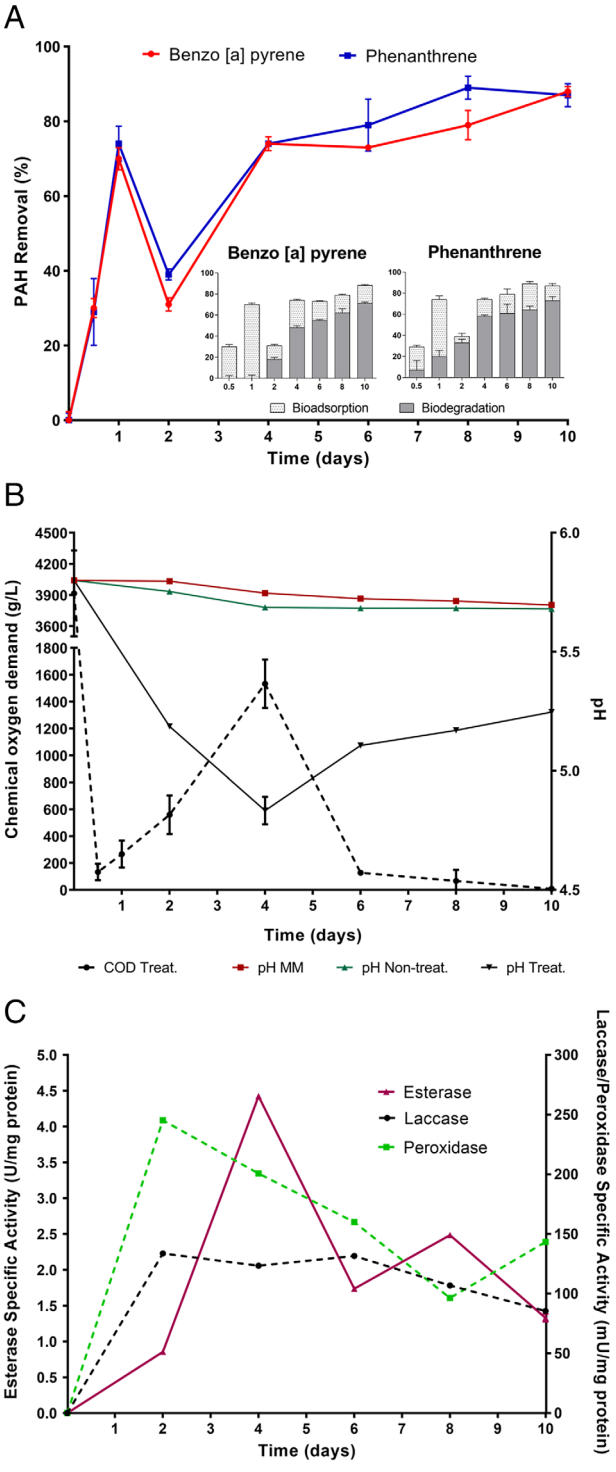

Fig. 1. Biochemical characterization of the polycyclic aromatic hydrocarbon (PAH) degradation process in *Aspergillus sydowii* exposed to hypersaline conditions.
A. Time-course analysis of benzo [*a*] pyrene and phenanthrene removal. Insets depict the contribution of bioadsorption and biodegradation to the total removal of each PAH.
B. Chemical oxygen demand (COD) and pH of the culture supernatant during the time-course of PAH degradation.
C. Manganese peroxidase, laccase and esterase activities in the culture supernatant during PAH degradation. No enzymatic activities were detected in negative controls (glucose media). COD Treat: Chemical oxygen demand after fungal treatment. pH MM: pH values determined for the minimal medium. pH Non-treat: pH values of non-treated (non-inoculated) minimal medium supplemented with PAHs. pH Treat: pH values of minimal medium supplemented with PAHs treated with *A. sydowii*. [Color figure can be viewed at wileyonlinelibrary.com]

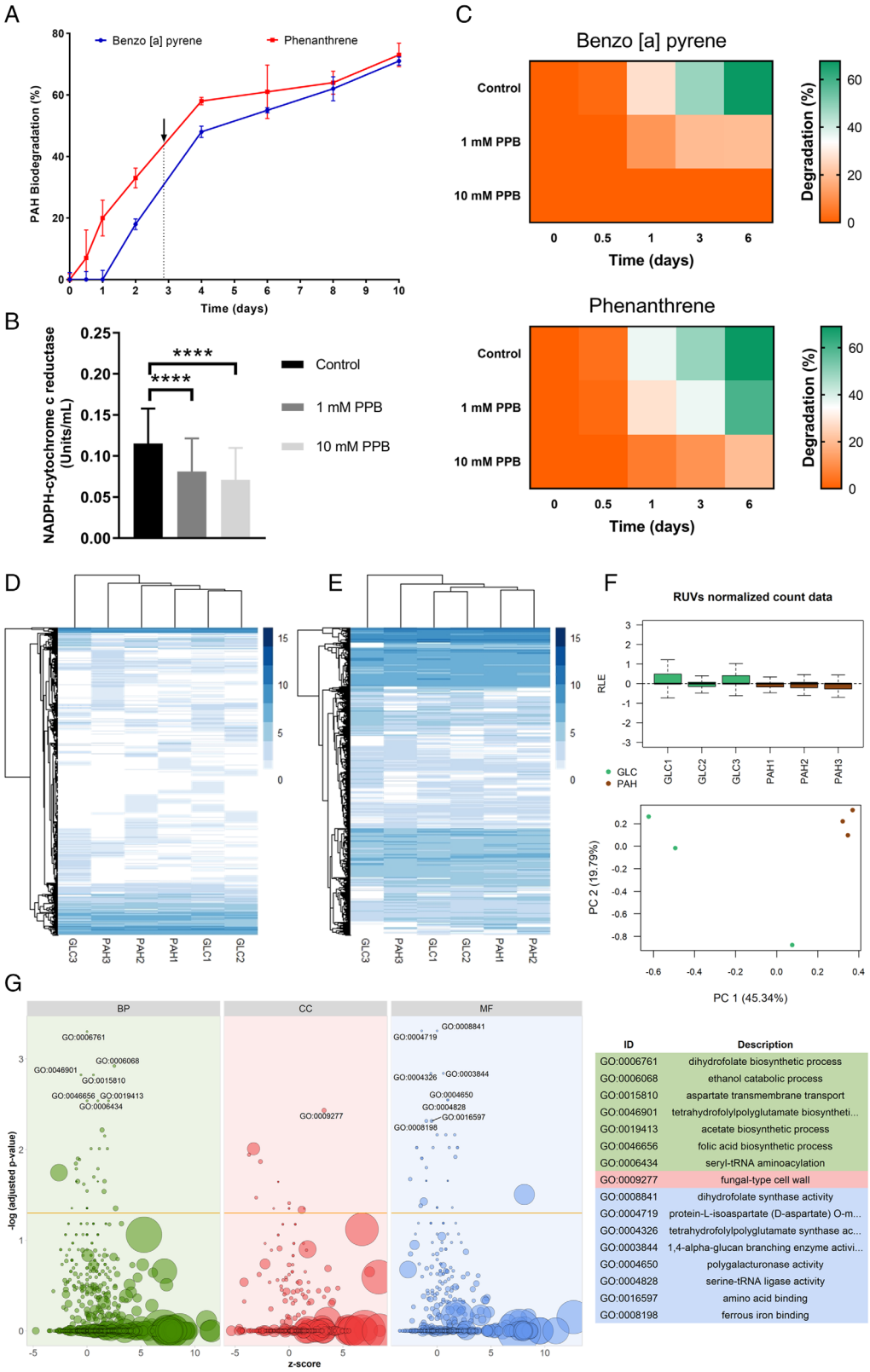

ID	Description
GO:0006761	dihydrofolate biosynthetic process
GO:0006068	ethanol catabolic process
GO:0015810	aspartate transmembrane transport
GO:0046901	tetrahydrofolylpolyglutamate biosyntheti...
GO:0019413	acetate biosynthetic process
GO:0046656	folic acid biosynthetic process
GO:0006434	seryl-tRNA aminoacylation
GO:0009277	fungal-type cell wall
GO:0008841	dihydrofolate synthase activity
GO:0004719	protein-L-isoaspartate (D-aspartate) O-m...
GO:0004326	tetrahydrofolylpolyglutamate synthase ac...
GO:0003844	1,4-alpha-glucan branching enzyme activi...
GO:0004650	polygalacturonase activity
GO:0004828	serine-tRNA ligase activity
GO:0016597	amino acid binding
GO:0008198	ferrous iron binding

Fig. 2. Legend on next page.

biodegradation (Fig. 2C). BaP biotransformation was strongly inhibited by PPB, as 1.0 mM PPB reduced its degradation by approximately 15% after the first day, while 10 mM PPB completely abolished the BaP biodegradation (Fig. 2C). Bioconversion of Phe also decreased, but to a lesser extent. These results suggest that *A. sydowii* degrades both Phe and BaP in part by a CYC-mediated mechanism.

After the biodegradative process was biochemically characterized, we focused our attention in transcriptomic analysis to identify molecular mechanisms involved in PAH biodepletion by the halophilic *A. sydowii*.

Transcriptome profiling in response to phenanthrene and benzo [a] pyrene degradation

To analyse *A. sydowii* transcriptome, the poly (A)-enriched mRNA samples were subjected to pair-end high-throughput Illumina HiSeq sequencing, resulting in 89 255 452 reads with an average length of 150 nucleotides (Supplementary Information Table S1). From the Trinity assembly, 33 560 contigs (also referred as transcripts) were obtained, corresponding to 28 751 possible genes (Supplementary Information Table S2). The expression profile of the samples (Fig. 2D) showed the prevalence of low count transcripts that could decrease the statistical power of the differential expression test. We thus applied a filter to eliminate the low read count transcripts (e.g. transcripts with counts per million (CPM) < 1.5 in more than three samples were eliminated), resulting in a set of 13 745 contigs used for subsequent analysis (Fig. 2E). This filtering step discarded transcripts that show low expression or consistency across samples, and eliminated expression data noise in the region of lowly expressed transcripts, allowing the distribution to better resemble a negative binomial distribution (as it is assumed by the differential expression method, DESeq2, used here) (Love *et al*., 2014) (Supplementary Information Fig. S1). Filtering of low read count transcripts also increases the statistical power of the test (Supplementary Information Fig. S1).

Hierarchical clustering of the expression profiles showed that the samples were not separated according to the treatment group (Figs 2D and E), indicating the need for further normalization to recover the separation into treatment clusters. After applying the RUVs (removal of unwanted variations) normalization method, all samples had homogeneous distributions of relative log expression (RLE) values and clustered as two different groups, as can be seen by the principal component analysis (Fig. 2F). The differential transcript expression analysis of *A. sydowii* growing with PAH as sole carbon source versus a control on glucose resulted in 170 upregulated and 76 downregulated genes (Supplementary Information Tables S3–S5). Gene ontology (GO) enrichment analysis of this set of differentially expressed (DE) transcripts showed that several biosynthetic processes were downregulated (Fig. 2G), as expected from the carbon source depletion induced by the PAHs treatment. GO related to ethanol catabolic pathway (GO: 0006068) was found enriched reflecting the changes of the carbon source. Interestingly, there was an increase in expression of genes associated with fungal cell wall remodelling, specifically the 1,4-alpha glucan branching enzymes, possibly reflecting the restructuring of the cell wall related to xenobiotics as external stimuli (Nishida *et al*., 2013). For example, in the solvent-tolerant *Saccharomyces cerevisiae* HK-211 has been well documented the upregulation of genes encoding cell wall proteins during solvent perturbation (Matsui *et al*., 2008; Nishida *et al*., 2013).

Most of the upregulated genes during PAH biodepletion encode proteins involved in degradation and metabolism of xenobiotics, cell detoxification, DNA/RNA metabolism, signalling and stress responses. Induction of genes implicated in mitochondrial functions (e.g. respiration and fatty acid oxidation) was observed, suggesting a drastic modification of the bioenergetic state of *A. sydowii* in the presence of Phe and BaP (Table 1). Besides, a carbonic anhydrase gene (*cah*) was also upregulated as a response to carbon starvation. *Cah* genes have key roles in other aspergilli during mineral nutrition under oligotrophic conditions as used in this study (Xiao *et al*., 2016; Loss *et al*., 2019).

The *A. sydowii* transcriptome upon exposure to PAHs revealed DE genes that might play important roles in xenobiotic metabolism, including chloroperoxidases (*cpo*), CYCs (*bc1, cyc, cox*), NADH ubiquinone oxidoreductases (*qr*), dioxygenases, dehydrogenases and glutathione-*S*-

Fig. 2. Transcriptome analysis of *Aspergillus sydowii* during the polycyclic aromatic hydrocarbon (PAH) degradation process.
A. Selection of transcriptome time-point in the time-course of the PAH biodegradation process. The arrow marks the selected time (day 3) for total RNA extraction.
B. Inhibition of NADPH-cytochrome *c* reductase by piperonyl butoxide (PPB) in the cells of *A. sydowii* at the time of RNA-Seq analysis.
C. Evaluation of the effect of cytochrome inhibition by PPB on the degradation of benzo [*a*] pyrene and phenanthrene.
D–F. Pre-processing of RNA-Seq data for differential expression analysis. Clustering of transcriptome profiles (D) before and (E) after filtering low read count transcripts. GLC, glucose.
F. Effect of remove unwanted variations (RUVs) normalization method on the relative logarithmic expression (RLE) (upper box), showing even distributions of expression across samples, and on the distribution of samples in a principal component analysis (lower box) showing clustering of treatment groups.
G. Gene ontology (GO) enrichment analysis on the set of differentially expressed genes during PAH degradation in *A. sydowii*. This graph was generated using GOplot version 1.02 (Walter *et al*., 2015). BP, biological processes; CC, cellular components; MF, molecular function. [Color figure can be viewed at wileyonlinelibrary.com]

Table 1. Differentially expressed genes involved in biodegradation and detoxification of polycyclic aromatic hydrocarbons (PAHs) by the halophilic fungus *Aspergillus sydowii*.

	Gene/transcript	Gene name	Protein ID	Transcript ID	logFC	FDR
Cytoplasmic pathway	Fructose bisphosphate	*fba2*	148295	148433	3.59	8.76E−06
	Thiol methyltransferase	*tmt*	88392	88530	1.88	2.82E−06
	Glutathione S-transferase	*gst*	89574	89712	1.71	1.45E−04
	3-Hydroxyanthranilate 3,4-dioxygenase	*bna1*	55821	55959	1.27	4.38E−02
	Short-chain dehydrogenase/reductase	*sdr*	89908	90046	1.25	9.58E−02
	Acyl-thioesterase II	*acot2*	38532	38670	1.19	4.61E−05
	Amino-acid N-acetyltransferase	*nat*	41645	41783	1.11	4.52E−02
	Carboxylesterase	*ces*	372617	372755	1.11	2.70E−02
	Chloroperoxidase	*cpo*	189715	189853	1.08	8.72E−02
	Vacuolar membrane PQ loop repeat protein	*pq*	509301	509439	1.03	5.61E−02
Mitochondrial pathway	FMN-dependent dehydrogenase reductase	*fdh*	35724	35862	1.67	8.08E−03
	Cytochrome c	*cyc*	39191	39329	1.21	5.87E−04
	Cytochrome *b-c1*	*bc1*	143844	143982	1.17	9.54E−02
	Cytochrome *c* oxidase	*cox*	54236	54374	1.17	5.79E−02
	NADH–ubiquinone oxidoreductase	*qr*	90079	90217	1.15	8.13E−02
Detoxification	Peptidylprolyl isomerase	*ppi*	146861	146999	1.16	4.06E−02
	Thioredoxin	*trx*	43391	43529	1.07	9.59E−02
	Nucleoside diphosphate kinase	*ndk*	508253	508391	1.06	4.20E−02

Gene name nomenclature is according to UniProt (https://www.uniprot.org). Protein ID and Transcript ID are according to the genome annotation of *Aspergillus sydowii* CBS 593.65 (De Vries *et al*., 2017). FC, fold change. logFC, fold change values expressed as $\log_2$ units. It provides a relative gene expression in polycyclic aromatic hydrocarbons versus glucose. FDR, false discovery rate.

transferases (*gst*), among others (Table 1). Only a *cpo* gene was upregulated among the extracellular enzymes capable of degrading PAHs. Chloroperoxidases are extracellular functional hybrids of heme peroxidase and CYP450 enzymes. They catalyse a wide variety of chemical reactions such as halogenations, dehalogenations, CYP450 dehydrogenations, as well as oxy and epoxygenizations (oxygen insertion) of double bonds in aromatic compounds (Wang *et al*., 2019). Chloroperoxidases can oxidize heterocyclic sulfides and oxidize PAHs such as dibenzothiophene (Vázquez-Duhalt *et al*., 2001). Interestingly, laccase genes (*lac*) did not exhibit changes in the expression level when *A. sydowii* grew in the presence of Phe and BaP.

Concerning the intracellular mechanisms involved in PAH assimilation, *bc1, cyc* and *cox* genes were also upregulated by Phe and BaP treatment. CYCs are capable of catalysing oxidative reactions and epoxidations, and have been investigated for their capacity to oxidase thiophenes and organic sulfides to sulphoxides (Sakaki, 2012). CYCs can also oxidase PAHs such as anthracene and pyrene, and catalyse the formation of anthraquinone and 1,8-pyrenedione (Kadri *et al*., 2016). The mycotreatment also induced NADH–ubiquinone oxidoreductase (*qr)* and 3-hydroxyanthranilate 3,4-dioxygenase (*bna1*) genes. Quinone oxidoreductases (e.g. NADH–ubiquinone oxidoreductase) catalyse the biotransformation of quinones into semiquinones, which are highly cytotoxic PAH byproducts (El-Najjar *et al*., 2011), while dioxygenases intervene to form dihydrodiols. In this study we identified the upregulation of dehydrogenase genes, e.g. *bna1*, short-chain dehydrogenase/reductase (*sdr*) and FMN-dependent dehydrogenase-reductase (*fdh*). Interestingly, esterase (e.g. carboxylesterase (*ces*) and acyl-thioesterase (*acot2*)) and protease [vacuolar carboxypeptidase (*cps*)] genes were also identified as DE. A putative *fmp46* mitochondrial redox gene, which could be required in the reduction of small toxic molecules, was also upregulated. Other DE genes were those encoding for glutathione-*S*-transferases, thio-methyltransferases and amino acid *N*-acetyl transferases, which combine with partially oxidized PAHs, glutathione, methyl groups and amino acids respectively (Thuillier *et al*., 2011).

One of the main causes of PAH toxicity is the induction of genome damage, possibly by intercalating in the DNA helix (Velmurugan *et al*., 2017). This effect is counteracted by the induction of repair and genome integrity maintenance mechanisms, some of which were observed in the cultures with PAH. For example, DNA repair exonuclease (*dre*), tyrosyl-DNA phosphodiesterase (*tdp*) and nucleoside diphosphate kinases (*ndk*) genes were upregulated. Other genes that play important roles in DNA recombination, mRNA expression/stability and in siRNA processing (e.g. *dnaj, mug134* and *trax*), as well as genes required in the transport of proteins and mRNA across the nuclear envelope (e.g. *tpr*), were also DE. Moreover, genes involved in the structure of chromatin in eukaryotic cells [e.g. histones H4 (*hh4*) and H2A (*hh2a*) genes] and a histone lysin or arginine demethylase gene (*jmjc*) were upregulated upon PAH exposure.

Finally, acetyl-CoA reductase (*acr*), acyl thioesterase (*acot2*) and thioredoxin (*trx*) genes were overexpressed. These are involved in the cellular response to maintain the cell's redox balance.

Identification of byproducts during phenanthrene and benzo [a] pyrene biodegradation

Metabolomics was employed to determine intermediate metabolites produced during the Phe and BaP biodegradation. Hydroxylated direct byproducts of PAHs (dihydroxy-Phe and hydroxy-BaP diol) were identified in the culture supernatant of *A. sydowii* after 3 days of incubation. Hydroxy-naphthoic acid and dihydroxy-benzene (catechol) were also detected. No aromatic metabolites were identified in culture supernatants after 10 days of culture. These results suggest that Phe and BaP are mineralized after 10 days of mycotreatment.

Morphological changes in A. sydowii *in response to polyaromatic conditions*

As stress conditions modify the micromorphology in fungi, we examined the morphological details of *A. sydowii* when exposed to polyaromatic stress (Fig. 3). Mycelium from medium with added glucose was characterized by a sustained polarized growth and complete septation (Fig. 3A and B). In the cultures with Phe and BaP hyphae exhibited isotropic swelling (Fig. 3C, D, G–N) and the presence of large vacuoles in subapical compartments (Fig. 3C–N), while apical compartments frequently displayed polarized growth (Fig. 3C, D, G–N). Additionally, hyphae were more branched than in the control cultures (Fig. 3C, D, G–I, L, M). Phe and BaP did not inhabit spore germination in the studied conditions (Fig. 3J, K, M).

Residual toxicity after mycotreatments: evaluation of different models

Residual toxicity after *A. sydowii* treatments was evaluated on the moss *Physcomitrella patens*, mononuclear cells from adult peripheral human blood (MCPB), and zebra fish (*Danio rerio*) to determine the safety of the metabolic intermediates obtained from both Phe and BaP. PAH mycotreatments by *A. sydowii* decreased the toxicity of the desalted synthetic media containing Phe and BaP on the different systems tested (Fig. 4).

Moss (*P. patens*) grown on medium exposed to PAH mycotreatment increased its growth rate by almost twofold in comparison to control without mycotreatment (Fig. 4A). The immunotoxicity of the treated media also decreased since TNF-α transcript levels were abolished approximately threefold when the PAHs were biodepleted by the fungus (Fig. 4B).

Toxicological analysis using zebrafish (*D. rerio*) embryo is ideal because of its small size and the facility to waterborne treatment. Embryos were grown with the treated media for 72 h; lethality, embryo development and defects in pigmentation were evaluated at 24, 48 and 72 h after supernatant exposure. At 24 and 48 h after treatment lethality was observed only the embryos treated with supernatant of day two, meanwhile a clear improvement in viability was observed with the supernatant treated from day four and onwards; the embryos with minimum media developed as the control embryos (Fig. 4C and D. Nevertheless, embryo viability evaluated at 72 h post-treatment was affected (Fig. 4E). The treated embryos showed a slight developmental delay at 24 h of treatment compared to the control (Fig. 4F). After 48 h of treatment, a clear effect on pigmentation was observed, mainly in embryos exposed to treated water from day two compared to control embryos; improvement in pigmentation was observed in the rest of the treated embryos (Fig. 4G and H).

Discussion

Biodepletion of phenanthrene and benzo [a] pyrene by A. sydowii

Many studies observed the potential of ascomycetous fungi, in particular, different species of the genus *Aspergillus* to metabolize PAHs (Sutherland and Cerniglia, 2010; Aranda, 2016). For example, *A. japonicus* was able to degrade up to 80% of PAHs present in soil after 14 days (Iheanacho *et al*., 2014), while *A. flavipes*, *A. fumigatus* and *A. terreus* assimilated from 13% to 45% of PAHs after 21 days (Pernía *et al*., 2012). Other promising species within the same genus were *A. sclerotiorum, A. ustus, A. niger* and *A. terricola* (Passarini *et al*., 2011; Godoy *et al*., 2016; Guntupalli *et al*., 2019; Teng *et al*., 2019). Recently, Loss and colleagues (2019) characterized the growth of *A. nidulans, A. flavus, A. oryzae* and *A. fumigatus* in the presence of BaP, convincingly showing that only live mycelium significantly removed it, as confirmed in this study for *A. sydowii*.

Aspergillus spp. is not the only ascomycetous genus with an outstanding capability to remove a wide range of highly cytotoxic PAHs. Other ascomycetes such as *Fusarium equiseti, Paecilomyces* sp., *Penicillium oxalicum, Penicillium pinophilum, Pestalotiopsis* sp., *Pseudollascheria boydii, Talaromyces verruculosus, Trichoderma asperellum* and *Trichoderma harzianum* have also shown a versatile ability to degrade PAHs (Kristanti and Hadibarata, 2015; Zafra *et al*., 2016; Aranda *et al*., 2017; Velmurugan *et al*., 2017; Gao *et al*., 2019).

High salinity could negatively affect PAH removal (Kargi and Dinçer, 2000; McGenity, 2010; Oluwadare *et al*., 2017). In the *A. sydowii* strain tested here the PAH biodegradation was not affected by 1 M NaCl salinity of the medium (González-Abradelo *et al*., 2019 and data not shown). This result is in agreement with Hidayat and colleagues (2012) who demonstrated that the chrysene biodegradation did not

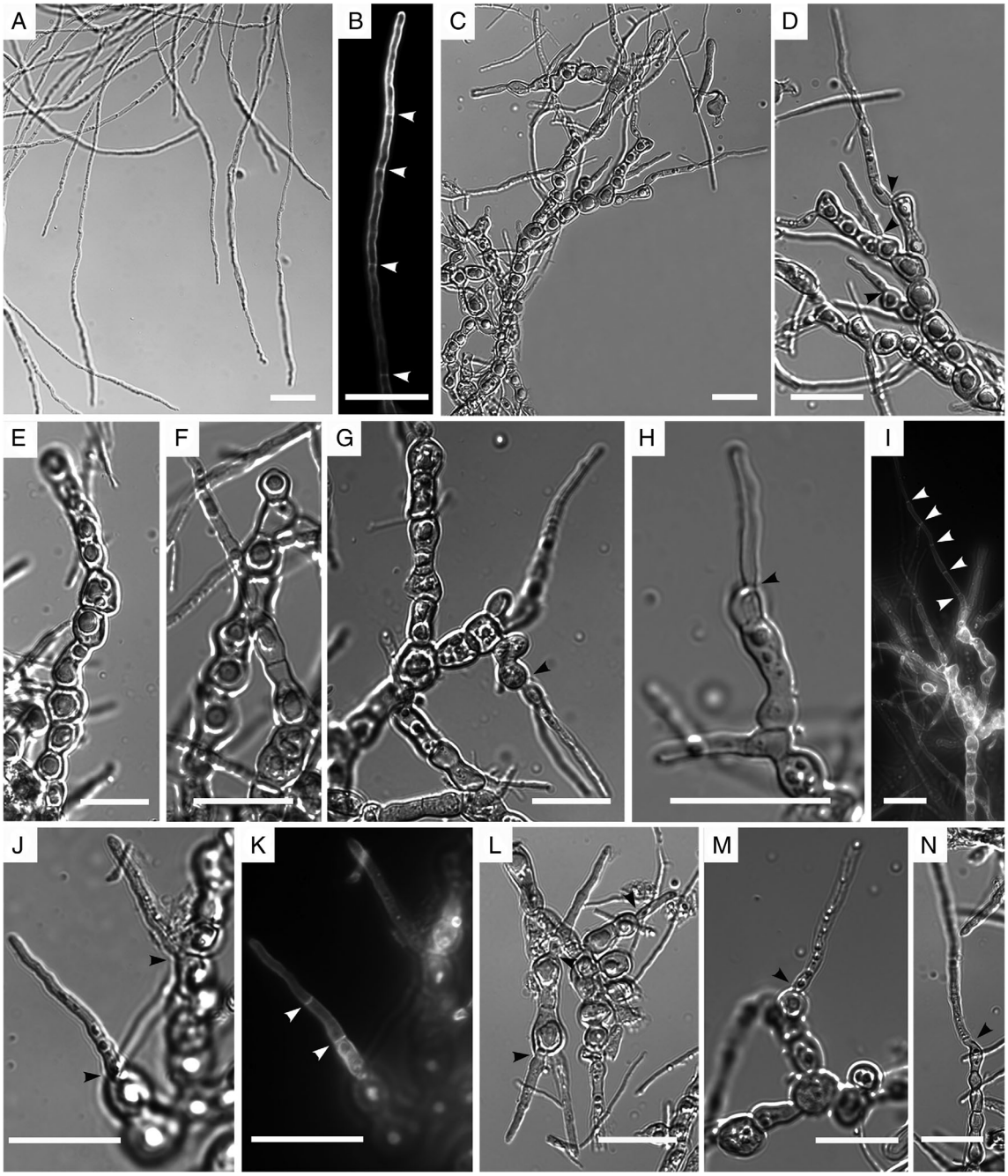

Fig. 3. Differential interference contrast microscopy of *Aspergillus sydowii* mycelium.
A and B. *A. sydowii*'s growth in the presence of glucose control. C–N. *A. sydowii*'s growth in the presence of benzo [*a*] pyrene and phenanthrene (PAH mixture, 1:1, 100 p.p.m. as final concentration). (A) Hyphae with polarized cell growth.
(B) Polarized hypha with completed septation (white arrows). (C–N) Hyphae (no polarized growth) with isotropic swelling cell growth and vacuolar expansion. Black arrows highlight apical compartments with polarized growth. White arrows remark septation. Scale bar: 20 μm.

change by the halotolerant *Fusarium* sp. F092 cultured under saline and nonsaline conditions. As evidenced for other microorganisms (Zafra and Cortés-Espinosa, 2015; Daccò *et al*., 2020; Yaguchi *et al*., 2020), the ecological origin of *A. sydowii* might affect its xenobiotic degrading capabilities. For example, a marine-derived strain of *A. sydowii* degraded only 30% of anthracene after 14 days in artificial seawater (~0.5 M NaCl) (Birolli *et al*., 2018), while our terrestrial strain showed a considerably higher PAH biodepletion.

Interesting, *A. sydowii* used in our study revealed a similar biotransformation profile for both Phe and BaP (Figs 1A and 2A) in spite of these PAHs exhibit different molecular weight,

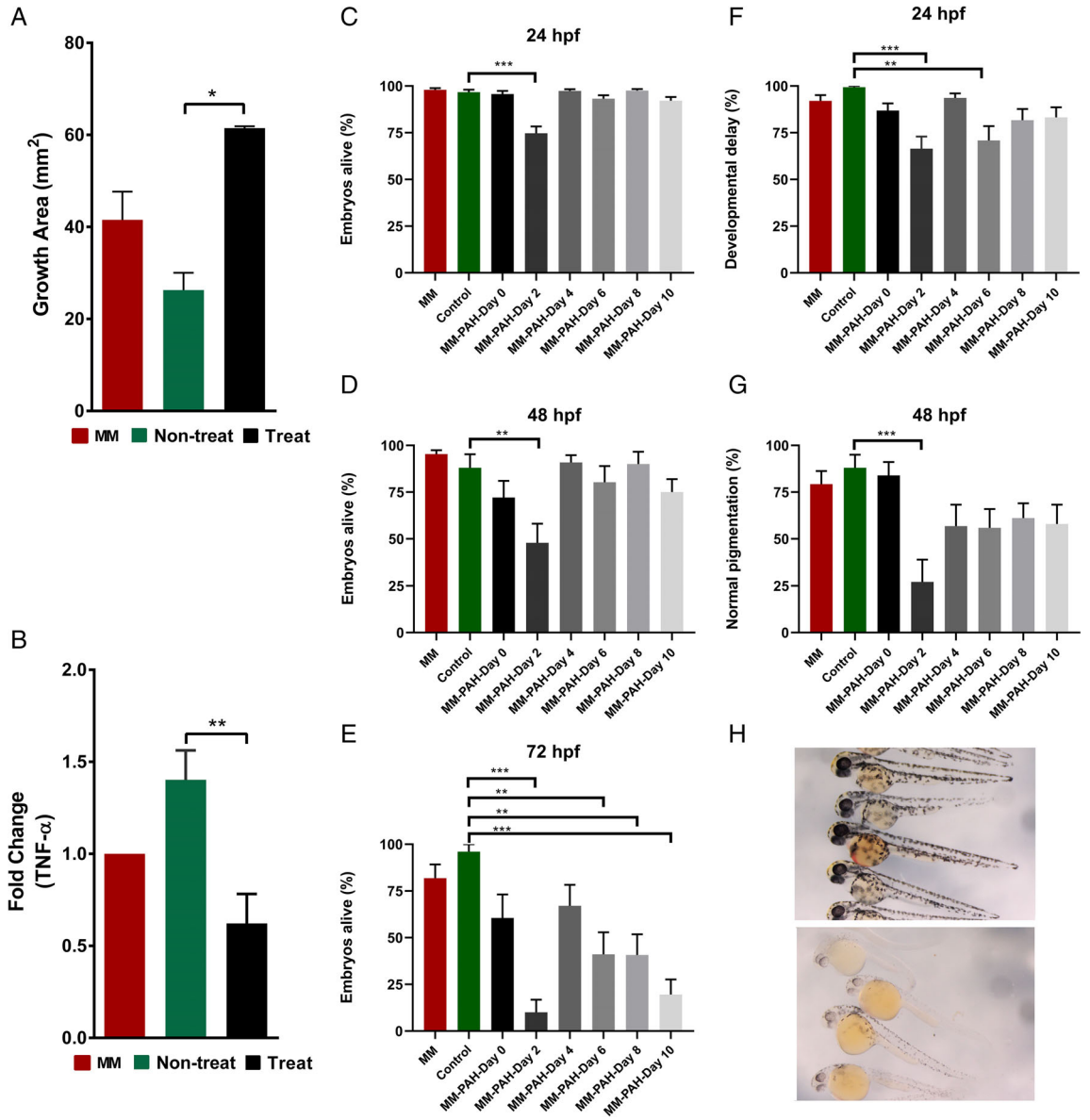

Fig. 4. Residual toxicity of polycyclic aromatic hydrocarbons (PAHs) in culture supernatant after *Aspergillus sydowii* treatment.
A. Evaluation of phytotoxicity by analysing relative growth rate of the moss *Physcomitrella patens* growing during 44 days in supernatants of PAH treated with *A. sydowii* (Treat), PAHs without *A. sydowii* (Non-treat).
B. Evaluation of toxicity to human cells by the production of tumour necrosis factor alpha (TNF-α) by mononuclear cells from adult peripheral blood (MCPB).
C. Zebrafish embryonic viability at 24 h of culture with supernatant from day 0 until day 10, statistical difference is observed at time point two compared to control or minimum medium (MM) (n = 2173).
D. Zebrafish embryonic viability at 48 h of culture with supernatant from day 0 until day 10, statistical difference is observed at time point two compared to control or minimum medium (MM) (n = 1131).
E. Zebrafish embryonic viability at 72 h of culture with supernatant from day 0 until day 10, statistical difference is observed at all time points compared to control or minimum medium (MM) (n = 1065).
F. Zebrafish embryonic development delay was measured at 24 h of culture with supernatant from day 0 until day 10.
G. Pigmentation is affected in the presence of PAHs at 48 h after culture with supernatant of day two mycotreatment compared to control media and further days of *A. sydowii* treated water. *p < 0.5, **p < 0.01, ***p < 0.001. H. Zebrafish embryos at 48 h of culture. Control embryos show normal pigmentation at this embryonic stage; meanwhile embryos treated with supernatant of mycotreated water with PAHs show a clear defect in pigmentation. Hpf, hours post fertilization. [Color figure can be viewed at wileyonlinelibrary.com]

aqueous solubility and ionization potential (Kadri *et al*., 2016). In counterpart Gao and colleagues (2019) reported preferential removal of Phe by *T. verruculosus*.

In the light of potential biotechnological applications of *A. sydowii* for bioremediation, it should be noted that changes in pH could serve as an indicator of PAH

degradation, relevant for further industrial scaling. However, not all reported ascomycetous fungi displayed similar pH changes during PAH assimilation. For example, pH gradually lowered in cultures of *A. fumigatus* during anthracene biotransformation (Ye *et al*., 2011), while in *P. oxalicum* it increased (Aranda *et al*., 2017), indicating different biomineralization strategies and degradation byproducts in different fungi.

The extracellular LME enzymatic activity profile did not correlate with the depletion of Phe and BaP during the 10 days of cultivation (Fig. 1C). Only at the beginning, the production of laccases and manganese peroxidases showed a similar trend that Phe and BaP conversions. No correlation ($r = 0.19$) between the activity of extracellular enzymes and assimilation of Phe and BaP was observed. This suggests the presence of additional (most likely intracellular) pathways for Phe and BaP degradation in *A. sydowii*. Similar results were found in *P. oxalicum* during anthracene metabolism (Aranda *et al*., 2017).

Transcriptomic insights on the polycyclic aromatic hydrocarbon degradation pathway in A. sydowii

The transcriptomic evidence of gene regulation during PAH biotransformation allowed us to propose possible polyaromatic compound degradation pathways in *A. sydowii*. Many of the metabolic steps in the PAHs degradation pathways are common for a wide range of microorganisms, from bacteria to algae, and are found even in plants (Oluwadara *et al*., 2017; Srivastava and Kumar, 2019). In contrast to Bacteria, where intracellular PAH degradation occurs by assimilation (they gain carbon and energy for growth), most fungi transform aromatic compounds by cometabolic processes (Prenafeta-Boldú *et al*., 2019). However, byproducts found in bacterial PAH degradation can also be found in fungi (Winquist *et al*., 2014). The main difference between fungal and bacterial metabolic pathways are the enzymes involved, as many transformations can be catalysed by several enzyme families. Accordingly, we propose that in *A. sydowii* two different pathways occur simultaneously (Fig. 5). The first named *'mitochondrial pathway'* involves membrane-bound enzymes from the mitochondria, including cytochromes, a CYC oxidase, respiratory chain dehydrogenases and a quinone reductase. The second pathway that was designated as *'cytosolic'*, involves soluble enzymes such as a dioxygenase, short-chain dehydrogenase reductase, thiol methyltransferase, glutathione transferase and fructose 1,6-bisphosphatase, among others. Although we envision that both pathways can effectively mineralize PAH, the most parsimonious mechanism is probably a combination of both where the intermediary metabolites shuttle from the mitochondria to the cytosol back and forth. Figure 5 shows all possible biotransformations of PAHs in *A. sydowii*, according to the identity of DE genes found in the transcriptomic analysis. The logFC values obtained for those DE genes involved in both biodegradative pathways are in agreement with those reported in other omics studies describing the proteomic response of *P. oxalicum* during anthracene biotransformation (Camacho-Morales *et al*., 2018).

Extracellular enzymes such as peroxidases and laccases have been extensively related to PAH conversion by fungi (Aranda, 2016; Oluwadara *et al*., 2017). The pattern of synthesized LME enzymes in *A. sydowii* (Fig. 1c) has been observed during the degradation of lignocellulosic biomass and other recalcitrant materials. Initially, fungi degrade lignin via laccases and peroxidases, followed by esterases when hemicellulose becomes more accessible. In the case of PAH assimilation, extracellular laccases and peroxidases might catalyse the enzymatic oxidation of phenolic rings, while the involvement of esterases is not fully understood. Since many ascomycetous fungi produce extracellular LME to induce the soft-rot decay of lignin, the secretion of esterases could be linked to the activation of evolutionary conserved regulatory mechanisms involved in lignocellulose degradation. Although esterase activity in the early stages of PAH mineralization has been reported for different fungi (Pozdnyakova *et al*., 2010; González-Abradelo *et al*., 2019), our transcriptomic data did not show overexpression of these genes in the presence of PAHs in *A. sydowii*. In contrast, high transcriptomic expression of laccases was observed previously in *Pleurotus ostreatus* in the presence of naphthalene (Elhusseiny *et al*., 2018), and in *T. verruculosus* in the presence of pyrene or Phe (Gao *et al*., 2019). Taken together, the transcriptional and enzymatic profiles of *A. sydowii* confirmed previous observations on the lack of correlation between LME production and PAH biodepletion in several ascomycetes (e.g. *Cadophora luteo-olivacea, Cladosporium, Lecythophora* and *P. oxalicum*) (Aranda *et al*., 2017).

To the best of our knowledge, this is the first transcriptomic evidence of the involvement of *cpo* genes during PAH degradation by fungi. Due to scarce information on the molecular level, their role in PAH biotransformation was so far poorly understood. It was hypothesized that chloroperoxidases could be particularly important in the extracellular degradation of high molecular weight PAHs (e.g. BaP), with a low diffusion coefficient for penetration through the cell membrane (Gao *et al*., 2019). A previous study of basidiomycetous *Phanerochaete chrysosporium* reported DE *cpo* genes when the fungus was grown in oak acetonic extract, indicating its potentially pivotal role in xenobiotic degradation (Thuillier *et al*., 2014). While peroxidase activity (e.g. total peroxidases, lignin- or manganese-peroxidases) was typically measured in many studies of fungal exposure to PAHs (Godoy *et al*., 2016; Aranda *et al*., 2017; Guntupalli

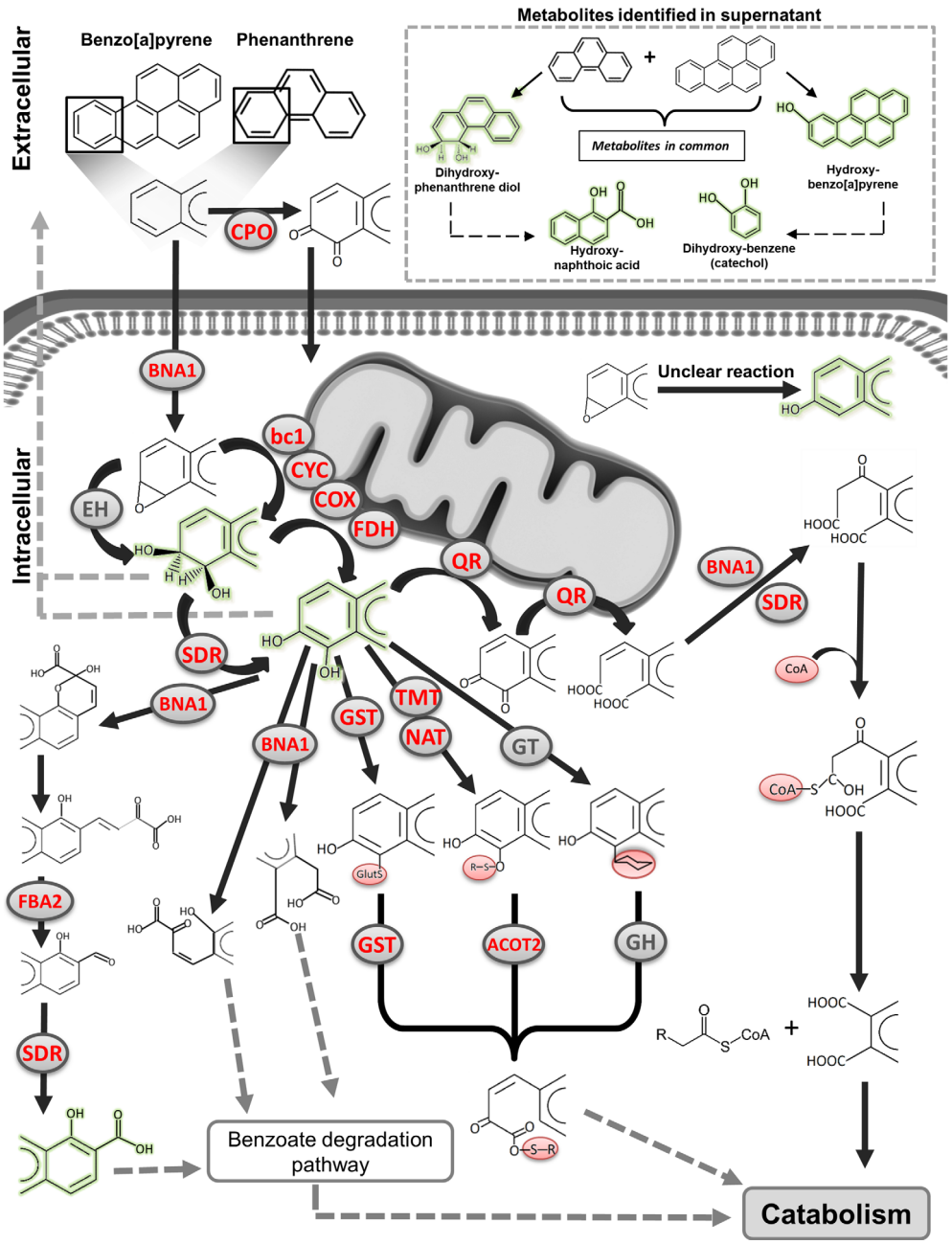

Fig. 5. Proposed pathways for the metabolism of benzo [*a*] pyrene and phenanthrene by *Aspergillus sydowii*. Transcripts for enzymes represented in red were found upregulated in the transcriptome analysis. Metabolites highlighted in green were identified in the culture supernatants on day three by ultra-high-performance liquid chromatography – mass spectrometry analysis. ACOT2, acyl-thioesterase II; bc1, cytochrome *b-c1*; BNA1, 3-hydroxyanthranilate 3,4-dioxygenase; COX, cytochrome *c* oxidase; CPO, chloroperoxidase; CYC, cytochrome *c*; EH, epoxide hydrolase; FBA2, fructose 1,6-bisphosphatase; FDH, FMN-dependent dehydrogenase reductase; GH: glycosyl hydrolase; GST, glutathione S-transferase; GST, glycosyl transferase; QR, NADH–ubiquinone oxidoreductase; SDR, short-chain dehydrogenase/reductase; TMT, thiol methyltransferase; NAT, amino-acid N-acetyltransferase. [Color figure can be viewed at wileyonlinelibrary.com]

et al., 2019), chloroperoxidase activity was not usually determined. Chloroperoxidase not only halogenate organic substrates susceptible to electrophilic attack but also possess oxygenase properties. In this way, they resemble CYP450-dependent monooxygenases, another member of the heme-thiolate proteins (Chen *et al*., 2014) that catalyse a multitude of oxygen transfer reactions (Urlacher and Schmid, 2004). Chloroperoxidase could be involved during mycoremediation in the transformation of PAH into quinone (Fig. 5) via peroxygenation (e.g., the oxygen originates from H_2O_2) (Manoj and Hager, 2001). This mechanism resembles the so-called 'peroxide-shunt'

in the catalytic cycle of CYP450 enzymes (Nordblom *et al*., 1976; Sundaramoorthy *et al*., 1995; Matsunaga *et al*., 2002; Denisov *et al*., 2005).

PAHs internalization is currently poorly understood in fungi. When anthracene, pyrene and BaP transporters were studied in *Fusarium solani*, only a passive hyphal PAH uptake, not correlated with a specific transport process or energy requirement was recognized (Verdin *et al*., 2005). In our study we did not identify any DE extracellular membrane transporter, suggesting that PAHs intake by *A. sydowii* mycelium occurs either via constitutive transporters or passively.

In the '*cytosolic pathway*' (Fig. 5), the initial intracellular oxidation step of PAHs could be catalysed by dioxygenase, resulting in the hydroxylation of two adjacent carbon atoms of the aromatic ring, thus generating a trans-dihydrodiol. This reaction converts hydrophobic, often toxic molecules, into more hydrophilic products, enabling subsequent metabolism by other enzymes (Gibson and Parales, 2000; Hernández-Ortega *et al*., 2015). Dioxygenases utilize NAD(P)H as a reductant and transfers electrons to the active site for dioxygen activation, a prerequisite to substrate hydroxylation (Hernández-Ortega *et al*., 2015). Both hydroxy-benzo [*a*] pyrene (mono- or di-hydroxylated) and phenanthrene-diol that were identified in *A. sydowii*, were also found in different ascomycetous and basidiomycetous fungi: *Armillaria sp., A. niger, Candida sp., Coriolopsis byrsina, P. chrysosporium, P. oxalicum, Pleurotus pulmonarius* and *Polyporus* sp. (Ning *et al*., 2010; Hadibarata *et al*., 2011; Hadibarata, 2013; Hadibarata and Chuang, 2014; Parshikov *et al*., 2015; Aranda, 2016; Kadri *et al*., 2016; Agrawal and Shahi, 2017; Aranda *et al*., 2017; Hadibarata *et al*., 2017; Birolli *et al*., 2018).

Afterwards the PAH trans-dihydrodiols are re-aromatized through short-chain dehydrogenase reductase to yield a dihydroxylated derivative, similar to catechol (Ghosal *et al*., 2016). Catechol can be transformed by a dioxygenase into a 2-hydroximuconic semialdehyde, that can be split into acetaldehyde and pyruvate to enter the tricarboxylic acid cycle (Fuchs *et al*., 2011). Similarly, the dihydroxylated PAHs can be transformed by a dioxygenase, mediating their incorporation into the benzoate degradation pathway. Interestingly, an intermediate of this pathway is the hydroxy-naphtoic acid, identified in the supernatant of *A. sydowii* (Fig. 5). The presence of catechol and naphthoic acid in the biodegradation of PAHs suggests elimination via dioxygenation and subsequent meta-cleavage, leading to PAHs mineralization, as observed in *Trichoderma sp*., *T. asperellum* and *Polyporus sp*. (Hadibarata *et al*., 2012; Zafra *et al*., 2015).

Dihydroxylated PAHs might be subsequently conjugated in the cytosol with thiols, glutathione, or monosaccharides, a process mediated by thiol-methyl transferase, amino acid *N*-acetyl transferase, glutathione-*S*-transferase and glycosyltransferase respectively (Fig. 5). Conjugation of PAHs serves various purposes from (i) water-solubilization that can facilitate their eventual elimination, to (ii) tagging involved in intracellular trafficking and storage, (iii) activation of the molecules for subsequent metabolic steps, or (iv) reduction of toxicity by preventing their interaction with proteins and nucleic acids (Verdin *et al*., 2005; Morel *et al*., 2013). In this regard, glutathione-*S*-transferases can catalyse the nucleophilic addition of reduced glutathione to electrophilic centres in organic compounds. The glutathione derivatives of PAHs have been identified as intermediates in PAH degradation (Dasari *et al*., 2018). On the other hand, thiol-methyl transferase catalyses the *S*-methylation of catechols (Cai *et al*., 2007), that can be transformed later by an acyl-thioesterase to the corresponding oxomethylthioether. Glycosyltransferases catalyse the transfer of glycosyl groups to a nucleophilic acceptor, with either retention or inversion of configuration at the anomeric centre, and the resulting conjugate can be transformed by a glycosyl hydrolase (non-DE) (Harms *et al*., 2011).

Alternatively, in the proposed *'mitochondrial pathway'* the PAHs oxidation could be catalysed by CYP-450 monooxygenases (non-DE) to form an arene oxide (Fig. 5), that in turn could be transformed into PAHs trans-dihydrodiols and dihydroxylated PAHs through the complexes CYC *bc1*, CYC *c* and cytochrome oxidase. These enzymes can perform hydroxylations of PAHs derivatives in the presence of hydrogen peroxide. Besides being involved in the electron transport system, they are also able to catalyse peroxidase-like reactions (Sakaki, 2012). In mitochondria, dihydroxylated PAHs can be transformed by quinone reductases into quinones and dicarboxylic PAH derivatives, toxic byproducts of PAHs degradation (Monks and Jones, 2002). Quinone oxidoreductases and dioxygenases were overexpressed in microbial communities inhabiting hydrocarbon polluted soils (Wang *et al*., 2016), supporting a possible role in PAH degradation. Dehydrogenase reductases have been also described as one of the enzymes capable of catalysing the conversion of quinones into hydroquinones (Hoffmann and Maser, 2007). The mRNA expression levels of *qr, sdr* and *bna1* genes were observed DE in PAH-supplemented cultures of *T. verruculosus* (Gao *et al*., 2019), while the proteome of *P. oxalicum* revealed DE the production of these enzymes in presence of anthracene (Camacho-Morales *et al*., 2018). Dicarboxylic PAH derivatives could be later combined with coenzyme A (CoA), and in a more soluble form, enter the catabolism.

The currently proposed fungal PAHs degradation pathway includes the oxidation by CYP450 monooxygenase

and the enzyme-catalysed hydration of the resulting arene oxide to yield trans-dihydrodiols by epoxide hydrolase. Genes encoding both enzymes were not DE in *A. sydowii* at the time point we analysed the transcriptome. Furthermore, this mechanism should be more complex as the metabolic intermediates are shuttled between the cytosol and the mitochondrial intermembrane space as previously mentioned.

cyc genes have been largely associated with PAH biotransformation in Ascomycota. Previous transcriptomic studies have demonstrated that *cyc* genes are upregulated during PAH biodepletion (Hernández-López *et al*., 2016; Huarte-Bonnet *et al*., 2018; Gao *et al*., 2019; Loss *et al*., 2019). For example, in *A. niger* a significant increase in the transcription level of *cyc* P450 genes during Phe exposure was observed (Huarte-Bonnet *et al*., 2018). Although it is generally recognized that CYP450 family plays pivotal roles in PAH degradation by fungi, a recent study indicated that CYCs other than CYP450s were employed in hydrocarbon assimilation (Huarte-Bonnet *et al*., 2018). In agreement, transcriptomic analysis in *A. nidulans* revealed that BaP induced no specific CYCs (Loss *et al*., 2019). *cyc c* gene, that was upregulated in *A. sydowii*, was downregulated when *T. verruculosus* grew in the presence of pyrene or Phe (Gao *et al*., 2019). These differences suggest that the transcriptional response of CYCs during PAH metabolization could be notably different in different fungi, reflecting their ecology and phylogenetic positions (Huarte-Bonnet *et al*., 2018).

The bioinformatic analysis of 11 phylogenetic neighbouring reference genomes of *A. sydowii* was performed to explore on the genomic level their ability to biodegrade PAHs (Fig. 6). Phylogenetically *A. sydowii* clusters with *A. nidulans* and *A. versicolor*, both well-known resilient xenobiotic degraders (Zhang *et al*., 2015). The *Versicolores* clade, where *A. sydowii* is currently placed, has the largest representation of aromatic ring-opening dioxygenases, laccases, acyl-coA thioesterase and cytochrome *c* oxidase in comparison with other investigated species. These expansions of genes suggest potential adaptations to aromatic compounds' degradation, representing an evolutionary selective advantage.

As present, transcriptomic studies of PAH bioassimilation in fungi are scarce in the literature (Hernández-López *et al*., 2016; Gao *et al*., 2019; Loss *et al*., 2019). When we included in our comparison all the publicly available transcriptional data associated with PAH degradation in fungi (Fig. 7), we unravelled different DE transcriptomic profiles in phylogenetically distant fungi, without a common pattern. We could conclude, however, that genes related to biodegradation, detoxification and self-defence mechanisms (e.g. DNA repair and redox balance maintenance) are DE under PAH bioassimilation. Other cellular processes (e.g. sugar catabolism and regulation, amino acid and nucleotide biosynthesis, reproduction and secondary metabolism) are affected as well. Further transcriptomic studies are needed to better elucidate perturbations and reprogramming of fungal cells when exposed to PAHs.

Detoxification and self-defence mechanisms upon polyaromatic exposure

Adsorption was one of the main cell responses to mitigate the PAH toxicity (Fig. 8). Phe and BaP, as well as the byproducts identified as metabolic intermediates in this study, can be easily adsorbed onto the mycelia cell wall due to hydrophobic interactions (Aranda, 2016). Above we analysed how thiol-methyl transferase, amino acid *N*-acetyl transferase and glutathione-*S*-transferase could be directly involved in PAH metabolic pathways. However, their unspecific function in maintaining the redox status of the cell (Thuillier *et al*., 2014) could explain as well their upregulation in these conditions. The transcriptomic analysis revealed that Phe and BaP induced the glutathione system in *A. sydowii* (Fig. 8). This important eukaryotic detoxification mechanism facilitates the efflux of certain highly cytotoxic PAH intermediate metabolites (Weisman *et al*., 2010; Lenoir *et al*., 2017). The system is mainly composed of glutathione-*S*-transferase, oxidized glutathione and glutathione reductases (Liu *et al*., 2017), probably involved in protection from oxidative stress (Morel *et al*., 2013). As shown in Fig. 8 this detoxification mechanism tags a variety of hydrophobic substrates with glutathione for transport into vacuoles or extracellular medium (Morel *et al*., 2013). Glutathione conjugates are intracellularly pumped into vacuoles by a vacuolar membrane PQ-loop repeat protein, where vacuolar serine carboxypeptidase and carboxylesterase play an important catabolic role. Also, glutathionylates could be extracellularly transported by glutathione pumps (Marrs, 1996; Morel *et al*., 2013) or pumped intracellularly by glutathione dependent multidrug resistant-associated proteins (Morel *et al*., 2013). Amino acid or sugar conjugates can be also transported by multidrug resistant-associated proteins (Fig. 8).

Among the genes involved in redox homeostasis, thioredoxins and xanthine dehydrogenases play a cytoprotective role against the oxidative stress caused by PAH assimilation (Hanschmann *et al*., 2013; Aranda, 2016) (Fig. 8). Accumulation of *acr* transcripts is also a signal of the oxidative damage that probably is induced by Phe and BaP in *A. sydowii*. On the other hand, *acot2* gene, implicated in the peroxisomal lipid metabolism, mitochondrial fatty acyl-CoA oxidation and subcellular trafficking of fatty acids (Tillander *et al*., 2017), was also found DE in the transcriptome.

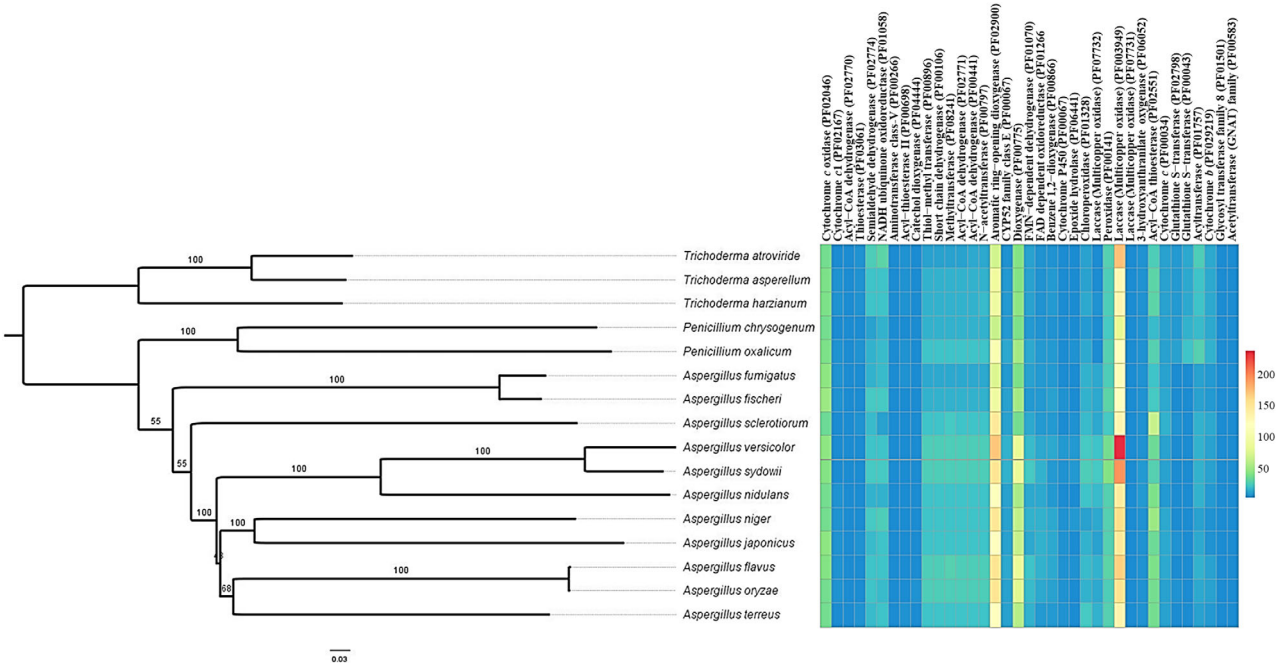

Fig. 6. Genome-based phylogenetic reconstruction for *Aspergillus sydowii* and close *Aspergillus* and *Penicillium* related species, associated with encoded sequences with a role on xenobiotic metabolism. *Trichoderma* clade was used as an outgroup. The tree was inferred with a concatenated protein alignment containing 42 837 sites. The heatmap illustrates the abundance of coding sequences gathered from genomic public annotations. The final version of the figure was generated using the GNU Image Manipulation Program GIMP 2.10.12. [Color figure can be viewed at wileyonlinelibrary.com]

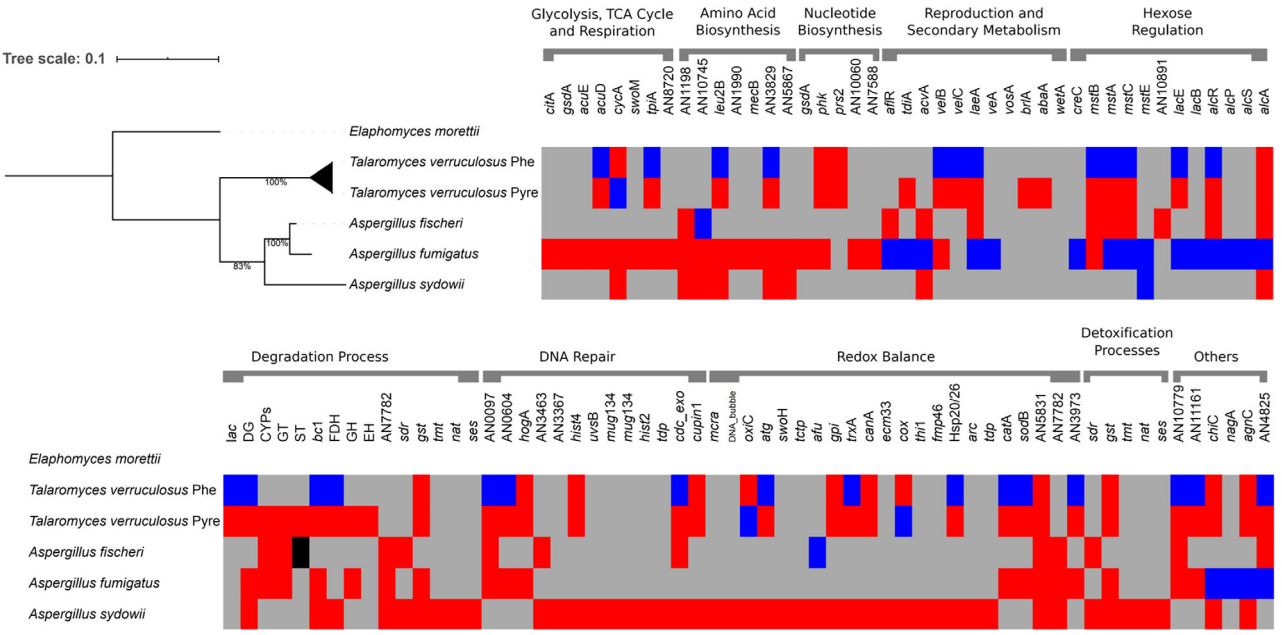

Fig. 7. Comparison of differentially expressed genes in publicly available transcriptional data associated with polycyclic aromatic hydrocarbon degradation in fungi. Transcriptional profiles from *T. verruculosus* (Gao *et al*., 2019), *Aspergillus fisheri* (Hernández-López *et al*., 2016), *Aspergillus fumigatus* (Loss *et al*., 2019) and *Aspergillus sydowii* (this study) were included in the analysis. [Color figure can be viewed at wileyonlinelibrary.com]

This observation is in accordance with studies reporting that reactive oxygen species produced by PAH metabolism cause lipid peroxidative injury (Singh *et al*., 2007; Gao *et al*., 2019). Our results are in agreement with studies performed in other fungi, reporting that genes mediating repair of oxidative damage were upregulated during PAH biodepletion (Thuillier *et al*., 2014; Velmurugan *et al*., 2017; Camacho-Morales *et al*., 2018;

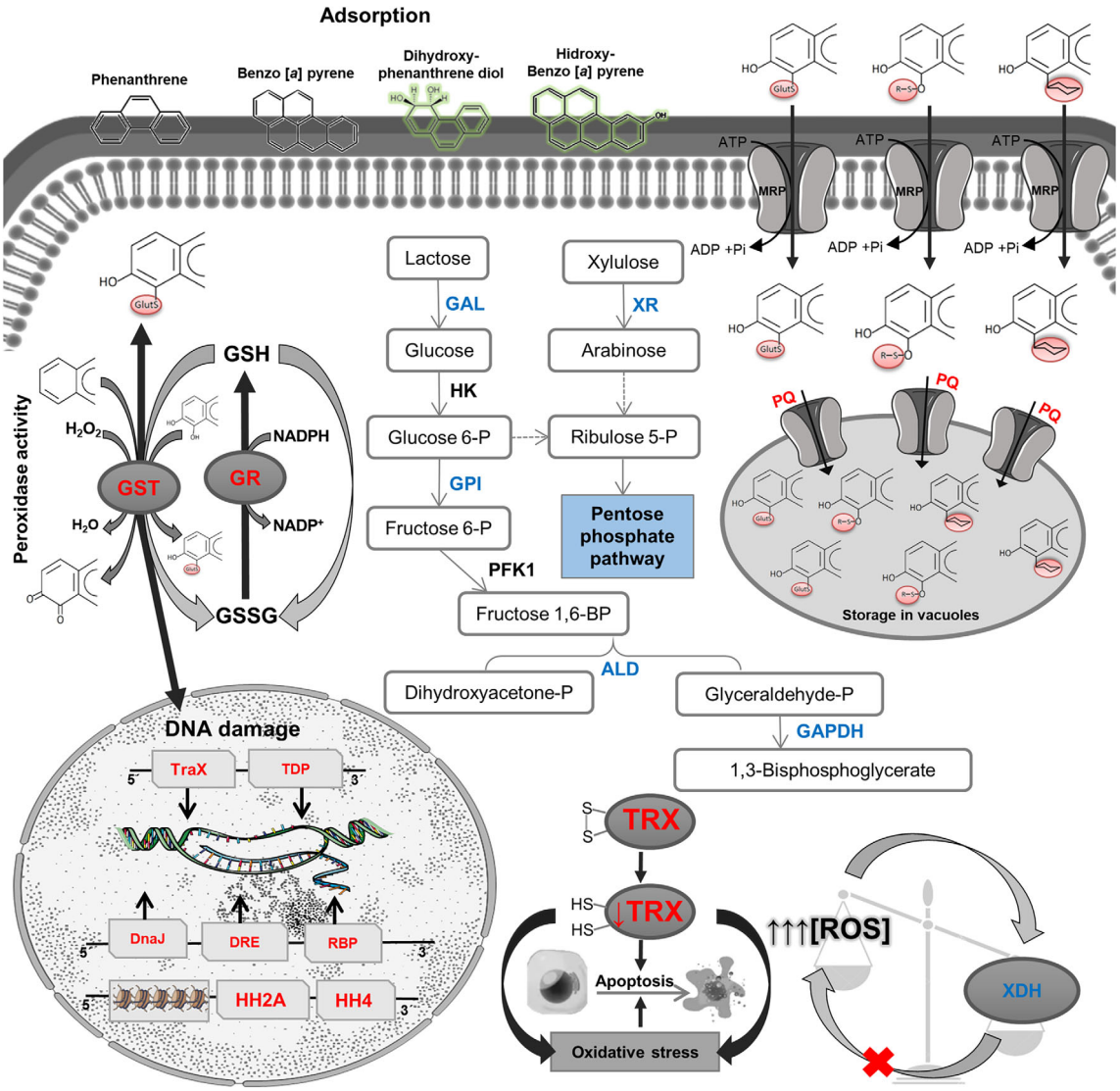

Fig. 8. Proposed mechanisms of tolerance to polycyclic aromatic hydrocarbon-induced stress, nutrient depletion, genotoxicity and reactive oxygen species (ROS) production in the cells of *Aspergillus sydowii* upon exposure to benzo [*a*] pyrene and phenanthrene. Transcripts for enzymes or proteins represented in red (blue) were found upregulated (downregulated) in the transcriptome analysis. Metabolites highlighted in green were identified in the culture supernatants on day three by ultra-high-performance liquid chromatography – mass spectrometry analysis. ALD, aldolase; ATP, adenosine triphosphate; DnaJ, chaperone DnaJ, also known as heat shock protein 40 kD. It is involved in cellular stress; DRE, DNA repair exonuclease; GAL, galactosidase; GAPDH, glyceraldehyde 3-phosphate dehydrogenase; GPI, glucose phospoisomerase; GR, glutathion reductase; GSH, glutathion; GSSG, oxidized glutathion; GST, glutathione S-transferase; HH, histone; HK, hexokinase; MRP, multidrug resistance-associated protein (transporter); Pi, pyrophosphate; PQ, vacuolar membrane PQ loop repeat protein; PFK1, phosphofructose kinase; RBP, RNA binding protein; TDP, tyrosyl-DNA phosphodiesterase; TraX, DNA-binding protein; TRX, thioredoxin; XDH, xanthine dehydrogenase; XR, xyloluse reductase. [Color figure can be viewed at wileyonlinelibrary.com]

Loss *et al*., 2019). In contrast, we did not find DE genes encoding for catalases (*cat*) and superoxide dismutases (sod) as in studies on *A. nidulans, Paecilomyces* sp., *P. chrysosporium* and *P. oxalicum*, when grown in the presence of xenobiotics (Thuillier *et al*., 2014; Velmurugan *et al*., 2017; Camacho-Morales *et al*., 2018; Loss *et al*., 2019).

A gene encoding carbonic anhydrase was also over-expressed during PAH treatment in *A. sydowii*. Carbonic anhydrase catalyses the hydration of CO_2 and has an important role in ion transport, acid–base balance and acid–base transport. CO_2 sensing is a crucial process to enhance the survival and proliferation in hostile growth conditions (Xiao *et al*., 2016; Loss *et al*., 2019) (e.g. PAHs as a sole carbon source). Carbonic anhydrases in *A. nidulans* play important roles responding to environmental changes, and acquiring mineral nutrition (Xiao *et al*., 2016; Loss *et al*., 2019), similar to conditions used in this study.

Taken together, the upregulation of the e.g. thiol-methyl transferase (*tmt*), amino acid *N*-acetyl transferase (*nat*), *gst*, glutathione reductase (*gr*), *trx, acot2* and *cah* genes reflects the activation of detoxification and self-defence mechanisms in *A. sydowii* when exposed to Phe and BaP (Fig. 8).

It is known that PAHs induce genotoxic damage and epigenetic alterations. Reactive intermediates produced during Phe and BaP biodegradation can covalently bind DNA forming PAH-DNA adducts, which increase the likelihood of gene mutations. Moreover, BaP induces genomic methylation disrupting the DNA methylation patterns in eukaryotes (Velmurugan *et al*., 2017). The *A. sydowii* transcriptomic analysis revealed an upregulation of certain genes involved in the DNA repair mechanisms, genome integrity and the expression and stability of mRNA. For example, *tdp* (DE gene in *A. sydowii*) removes a variety of covalent adducts from DNA, needed to repair DNA double-strand breaks caused by free radicals (Kawale and Povirk, 2018). DNA damage responses were upregulated also in PAH-treated mycelium of *A. nidulans, Paecilomyces* sp. and *P. oxalicum* (Velmurugan *et al*., 2017; Camacho-Morales *et al*., 2018; Loss *et al*., 2019). In addition, Phe and BaP affected in *A. sydowii* the nuclear trafficking of proteins and mRNA since *trp* genes were overexpressed. The upregulation of *jmjc* genes demonstrated that PAHs may cause epigenetic perturbations. *Jmjc* genes are involved in histone methylation, notably affecting the regulation of gene expression (Klose *et al*., 2006). Finally, genes implicated in the cell cycle control [peptidyl-prolyl isomerase (*ppi*) gene] were also overexpressed in *A. sydowii*. These genes influence transcriptional regulation and were found DE in the proteome of *Pseudomonas fluorescens* during naphthalene degradation (Herbst *et al*., 2013). In summary, our results suggest that Phe and BaP induced genotoxicity in *A. sydowii* (Fig. 8), counterbalanced by a marked increase in the level of mRNA related to DNA repair mechanisms, helping to maintain genome structure, preventing extensive DNA damage, regulating transcription and controlling cell fate. Molecular mechanisms that explain in more detail how PAHs affect the expression and regulation of the genetic information need further clarifications.

Figure 8 summarizes the detoxification response and self-defence strategies upon PAH exposure in *A. sydowii* under hypersaline conditions, as well as the transcriptional regulation of certain enzymes involved in the carbohydrate metabolism.

Residual toxicity after mycotreatments by A. sydowii

For the evaluation of the diminished toxicity of media after mycotreatment with *A. sydowii* different model organisms were used. Our results demonstrated that mycoremediation decreased toxicity.

There is abundant evidence that PAHs are toxic to several flowering plant species affecting their germination (Maila and Cloete, 2002), reducing their root growth, leaf number and size and inducing stress responses (Alkio *et al*., 2005). Non-vascular plants, such as mosses, are due to their simple anatomy even more sensitive to xenobiotics and therefore widely used as bioindicators of soil, air and water pollution (Cortis *et al*., 2016; Pradhan *et al*., 2017). In this study we used the moss *P. patens*, to determine the efficiency of *A. sydowii* in reducing PAH toxicity. Previous toxicity analysis of the effects of PAHs, specifically Phe and fluorene, on *P. patens* physiology demonstrated that 0.5 μM Phe decreased its photosynthetic activity during the first 48 h of exposure and that *P. patens* synthesizes glutathione as part of its defence strategy (Burritt *et al*., 2008). These defence mechanisms could explain the slightly negative effect of PAH on *P. patens* during our assay. It should be noted, however, that mycotreatment with *A. sydowii* generally showed a positive impact.

Also, the residual toxicity also exhibited an important reduction on human cells according with the TNFα factor levels expressed by MCPB exposed to supernatants after mycotreatment. It has been well documented that PAHs induce immunotoxicity, proinflammatory responses and carcinogenesis (Wang *et al*., 2017). For this reason, we used TNFα as a bioindicator molecule of immunotoxicity after mycotreatments.

The zebrafish (*D. rerio*) have been well established as a model to test the effects of diverse pollutants in toxicological studies (Ali *et al*., 2011; Qiang and Cheng, 2019). Treatment of zebrafish embryos with the supernatants after mycotreatment showed a time dependent effect on viability and developmental delay. Interestingly embryos showed only statistical differences with respect to viability and pigmentation at 24 and 48 h after treatment only with supernatants from day two compared to control water. No statistical difference was observed at the beginning of the treatment, possibly to the fact that the first day of culture PAHs are mainly absorbed onto the mycelium. We observed a clear effect in viability, development and pigmentation when the degradation of the PAHs commences after 2 days of treatment with *A. sydowii*; these effects were reduced when embryos were exposed to the water treated from day four onwards. Defects in pigmentation at 48 h treatment with water of day two of culture suggest that the accumulation of byproducts identified in the culture supernatant of *A. sydowii* could affect normal accumulation of melanin. Embryos cultured on PAH mycotreatment water developed normally, showing that the PAH treatment with *A. sydowii* is effective in reducing PAHs toxicity. Nevertheless; viability was clearly affected

after 72 h of culture with the mycotreated supernatants; this finding suggests that even very small amounts of PAHs can impair embryonic development, making zebrafish model a very sensitive assay for detection of water pollutants; further characterization of byproducts in media should be addressed.

Final remarks

Mycoremediation is increasingly recognized as an eco-friendly method for removal of some toxic, carcinogenic, mutagenic and persistent compounds from aquatic ecosystems. However, the molecular mechanisms of these processes are little known and transcriptomic studies are scarce.

In this study we show that halophilic *A. sydowii* is able to remove two of the most important organic pollutants, Phe and BaP (PAHs), from hypersaline aquatic environments. This process was followed by growth and enzymatic analysis with particular focus on extracellular lignin modifying enzymes (LME). The LME activity profile did not correlate in time with the depletion of Phe and BaP. Removal of PAHs was mediated by metabolic enzymatic transformation by the living mycelium, and not due to adsorbtion by the dead mycelium. As one of the first reported transcriptomic analyses of *Aspergillus*, we have used these to gain additional insight into metabolic detoxification. When *A. sydowii* was exposed to toxic stress and starvation due to PHAs as sole carbon sources, twice as many genes were upregulated as downregulated compared to growth on glucose. Due to starvation related to the presence of PAHs as sole carbon sources, several biosynthetic processes were downregulated (e.g. sugar catabolism and regulation, amino acid and nucleotide biosynthesis, reproduction and secondary metabolism). Upregulated genes were related to changes of the carbon source (e.g. *cah* gene as a response to carbon starvation), cell wall remodelling, degradation and metabolism of xenobiotics, cell detoxification, DNA/RNA metabolism, DNA repair genes and genome integrity maintenance, energy metabolism (e.g. respiration and fatty acid oxidation), signalling and general stress responses. LME, previously considered important for PAH biotransformation, did not change expression levels. On the other hand, we identified for the first time upregulation of a *cpo* gene, indicating that this enzyme could play an important role during PAH degradation by fungi. Based on transcriptomic analyses we propose two parallel pathways for polyaromatic compound degradation in *A. sydowii*: mitochondrial and cytosolic. The mitochondrial pathway involves membrane-bound enzymes from the mitochondria, including cytochromes, a CYC oxidase, respiratory chain dehydrogenases and a quinone reductase. The cytosolic pathway involves soluble enzymes such as a dioxygenase, short-chain dehydrogenase reductase, thiol methyltransferase, glutathione transferase and fructose 1,6-bisphosphate, among others.

Comparison of our results with other transcriptomic studies and bioinformatics analyses of 11 *Aspergillus* reference genomes illuminates the widely spread ability to biodegrade PAHs in genus *Aspergillus* and other fungi. Further transcriptomic and proteomic studies are needed to elucidate perturbations and reprogramming of fungal cells when exposed to PAHs. We expect such knowledge to help us using and focusing the methods in our toolbox (such as screening, mutation, gene manipulations) to improve the ability of selected strains of *Aspergillus* to degrade toxic substances – also under extreme conditions. Our ultimate goal is to help unlock the enormous potential of extremophile fungi for bioremediation purposes.

Experimental procedures

Strain and culture conditions

A. sydowii EXF-12860 is a halophilic fungus isolated from sugarcane bagasse supplemented with 2 M NaCl (Batista-García *et al*., 2014). The strain was preserved in 20% glycerol at −80°C and deposited in the Ex Culture Collection of Extremophilic Fungi at the Infrastructural Centre Mycosmo, at the Biotechnical Faculty, University of Ljubljana, Slovenia. Fresh spores and mycelium were obtained from cultures on Malt Extract Agar (MEA) with added 1 M NaCl.

A pre-inoculum culture of *A. sydowii* was obtained in liquid medium by inoculating 1×10^6 spores into 250 ml flasks containing 50 ml of Minimal Medium (MM) supplemented with 2% glucose and 1 M NaCl. The composition of the MM was: 7.8 mg l^{-1} $CuSO_4{\cdot}5H_2O$, 18 mg l^{-1} $FeSO_4{\cdot}7H_2O$, 500 mg l^{-1} $MgSO_4{\cdot}7H_2O$, 10 mg l^{-1} $ZnSO_4{\cdot}7H_2O$, 50 mg l^{-1} KCl, 1 g l^{-1} K_2HPO_4, 2 g l^{-1} NH_4NO_3, 2 g l^{-1} KH_2PO_4, 100 mg l^{-1} $CaCl_2$, 5 mg l^{-1} $MnSO_4$, 0.1 mg l^{-1} H_3BO_3, 0.1 mg l^{-1} $NaMoO_4{\cdot}2H_2O$ and 1 mg l^{-1} $CoCl_2$. Culture was incubated at 28°C and 150 r.p.m. until reaching the exponential growth phase (4 days). Later, mycelium was collected by centrifugation at 4000*g*, at 4°C for 10 min and washed three times with saline solution (0.5% NaCl). To deplete the nutrients accumulated in the fungus after its growth in the glucose-supplemented medium, 3 g of mycelium was transferred into 250 ml flasks containing 50 ml of MM with 0.5% NaCl and incubated for 18 h at 28°C and 150 r.p.m. Subsequently, the mycelium was collected as previously described and 1 g was inoculated in 250 ml flasks containing 30 ml of MM, 1 M NaCl with a mixture of 50 p.p.m. benzo [*a*] pyrene (BaP) (Sigma–Aldrich, Catalogue

No. B1760, St. Louis, USA) and 50 p.p.m. phenanthrene (Phe) (Sigma–Aldrich, Catalogue No. P11409, St. Louis, USA), 100 p.p.m. total concentration. Cultures were incubated at 28°C and 150 r.p.m. during 10 days.

For the evaluation of PAHs removal, culture flasks were removed after 0, 0.5, 1, 2, 3, 8 and 10 days. Total removal, bioadsorption and biodegradation of BaP and Phe were determined at each sampling time. Non-inoculated flasks with and without PAHs were included in the experiment as negative and positive controls respectively. Cultures were made in triplicates for each experimental time point. Three independent experiments were conducted (total $n = 9$ per time point).

For transcriptome analysis, fungal mycelium was collected after 3 days of exposure to PAHs. In addition, a control culture was incubated at similar conditions, but transferred in the end into MM supplemented with 2% glucose and 1 M NaCl. Three independent cultures were obtained for each condition.

Quantification of benzo [a] pyrene and phenanthrene

Culture supernatant and mycelium were separated by centrifugation at 4000*g* and 4°C for 10 min. BaP and Phe were recovered through organic solvent extraction using 2 ml of mass-spectrometry grade hexane. Three consecutive extractions were performed using 2 ml of supernatant or 1.5 g of wet mycelium. Six millilitres of hexane were recovered and later concentrated six times using a rotary vacuum evaporator. Gas chromatograph–mass spectrometer (GC–MS) was employed to determine quantitatively BaP and Phe according to Lee and colleagues (2010, 2014). Briefly, PAH separation was performed on a G1800A GC (Hewlett-Packard, Palo Alto, CA) by using an HP-5 MS fused-silica column (30 m × 0.25 mm i.d., 0.25 mm film thickness) (Hewlett-Packard) and coupled to an electron ionization detector. All experimental determinations were performed in triplicate for each sample. The removal of PAHs was calculated as the difference between the PAHs in the supernatant of mycelial treatment and the mean PAH concentration in negative controls. Bioadsorption was considered as the BaP and Phe quantified in the mycelium fraction. Biodegradation was calculated as the difference between the mean of PAHs in negative controls and the total amount of PAHs in supernatant and mycelium.

Enzymatic activity assays

Laccase and peroxidase activities were measured by the oxidation of 2,2′-azino-bis(3-ethylbenzothiazoline-6-sulphonic acid) (ABTS) (1 mM) (Sigma–Aldrich, Catalogue No. A1888, St. Louis, USA) at 420 nm ($\varepsilon = 3.6 \times 10^4\ M^{-1}\ cm^{-1}$) in 0.1 M citric acid/0.1 M disodium hydrogen phosphate buffer at pH 5, according to Touahar and colleagues (2014). For peroxidase activity the same protocol was used with the addition of H_2O_2 (0.005%). Esterase activity was measured by following the conversion of 2-naphthyl-acetate (Sigma–Aldrich, Catalogue No. N6875) to naphtol ($\varepsilon = 23{,}395\ M^{-1}\ cm^{-1}$) at 538 nm (Batista-García *et al*., 2014). Cytochrome c reductase (NADPH) activity was measured using a Cytochrome *c* reductase (NADPH) assay kit (Sigma–Aldrich, Catalogue No. CY0100, St. Louis, USA) according to the manufacturer's instructions. UPO activity was measured according to Camacho-Morales and colleagues (2018). One International Unit (IU) of enzymatic activity was defined as the amount of enzyme per milligram of total protein catalysing the oxidation of 1 mmol of substrate per minute.

Cytochrome inhibition experiment

A pre-inoculum culture of *A. sydowii* was incubated, washed and collected as previously described and 1 g of mycelium was inoculated in 250 ml flasks containing 30 ml of MM, 1 M NaCl, 100 p.p.m. final concentration of BaP and Phe (1:1) and 1 mM or 10 mM of piperonyl butoxide (PPB) (Sigma–Aldrich, Catalogue No. 291102, St. Louis, USA) as cytochrome (CYC) inhibitor. Cultures were incubated at 28°C and 150 r.p.m. For the evaluation of CYC inhibition, culture flasks were removed after 0, 0.5, 1, 3 and 6 days. Non-inoculated flasks with PPB were included in the experiment as negative controls. Cultures were made in triplicates for each experimental time point. Subsequently, the supernatants were collected to proceeded with BaP and Phe quantification as previously described.

Microscopy of A. sydowii *in the presence of polyaromatic conditions*

Fungal samples exposed to BaP and Phe were observed using the inverted agar method (Hickey *et al*., 2004) in a NiKon Eclipse Ti-U microscope equipped with an Apo 60x/1.49 A.N. objective using a Hamamatsu Orca Flash 4.0 camera. Samples were fixed and stained with calcofluor white, and excited with a mercury lamp using ET-DAPI filters. Also, mycelium produced in presence of glucose was observed under the microscope.

Toxicological screening assays

Residual PAHs and possible intermediate metabolites were recovered as previously described from culture supernatants using organic solvent extraction with hexane. The organic extracts were evaporated up to 2 ml.

Organic extracts from non-inoculated MM with or without PAHs were included as negative and positive controls respectively.

To evaluate phytotoxicity, the moss *Physcomitrella patens* was grown on Knop solid medium (Reski and Abel, 1985) for 7 days at 22°C and 16 h light/8 h dark. The control was supplemented with hexane. Plants were grown during 44 days at 22°C and 16 h light/8 h dark. To analyse the relative growth of plants during treatment, the explants were photographed with a Nikon Colpix5000 camera at the beginning (day 0) and end (day 44) of the experiment. The area (mm^2) covered by plants was measured using ImageJ software (http://rsb.info.nih.gov/ij/). The relative growth rate was calculated according to Medina-Andrés and colleagues (2015).

Cytotoxicity to human cells was evaluated by the production of the tumour necrosis factor alpha (TNFα), a stress cytokine, by mononuclear cells from adult peripheral blood (PBMC) exposed to different volumes of the culture supernatant. PBMC were isolated by density centrifugation over Lymphoprep (Axis-Shield, Scotland). Monocytes were eliminated by plastic adhesion overnight. Cells were cultured in RPMI 1640 medium (Thermo Fisher, Catalogue No. 11875093, USA) supplemented with 2 mM glutamine, commercial antibiotics (50 U ml^{-1} penicillin, 50 mg ml^{-1} streptomycin) and 5% fetal bovine serum (Thermo Fisher, Catalogue No. 16140063, USA). The cells were stimulated for 6 h with the supernatants obtained after fungal treatment or with control media. Later, cells were pelleted and total RNA was obtained using TRIzol Reagent (Thermo Fisher, Catalogue No. 15596026, USA) method. One milligram of total RNA was used to obtain cDNA, using RevertAid Reverse Transcriptase and poly (I-C) (Thermo Fisher, Catalogue No. K1691, USA). TNFα transcript levels were measured by qPCR in a StepOne thermocycler (Applied Biosystems), using Maxima SYBR Green/ROX qPCR Master Mix (Thermo Fisher, Catalogue No. K0221, USA). Human glyceraldehyde 3-phosphate dehydrogenase (GAPDH) gene was used as a reference for normalization. The following primers were used for amplification: GAPDH, forward 5′ CCCCCGGTTTCTATAAATTGAGCCC 3′ and reverse 5′ AAATCCGTTGACTCCGACCTTCACC 3′; TNFα, forward 5′ CTGTAGCCCATGTTGTAGCAAAC 3′ and reverse 5′ ATGAGGTACAGGCCCTCTGAT 3′.

AB line and wild-type zebrafish (*D. rerio*) embryos were obtained from natural crosses and raised at 28°C based on standard procedures (Westerfield, 2000). Eggs were obtained by random pairwise mating of zebrafish. The eggs were harvested the following morning and transferred into plastic Petri dishes (60 eggs per dish) containing 10 ml fresh embryo water. Further, unfertilized, unhealthy and dead embryos were identified under a dissecting microscope and removed. Embryonic stages were determined by morphological criteria according to Kimmel and colleagues (1995). Zebrafish were handled in compliance with local animal welfare regulations, and all protocols were approved by the Comité de Ética (Instituto de Biotecnología, UNAM).

At 3.5 h post fertilization, embryos were again screened, and any further dead and unhealthy embryos were removed. Embryos at sphere stage were selected and transferred into a 48 well plate; 10 embryos per well. Later the embryo water was absorbed and 300 µl of water supernatant was loaded in each well; experiments were done in triplicate with triplicates for each experimental time point and three independent experiments were carried out. As a control, a set of embryos were grown with embryonic water in the same plate but also in a petri dish independently. The plates were cultivated in a moist chamber at 28°C from 24 h to 72 h and the viability developmental delay and pigmentation of the embryos was observed under a dissecting microscope. Embryos were anaesthetised with tricaine, immobilized with methylcellulose on agar plates and visualized with a stereomicroscope (Leica MZ 12.5, Zeiss, Germani), photographed using a CCD camera (AxioCam MRc 5, Zeiss, Germani) and the AxioVision Rel. 48 software. Statistical analysis was performed with three independent experimental replicates. The exact number of biological replicates is indicated in the figure legends. Statistical analysis was performed with Prism (GraphPad, San Diego, CA, USA) Student's *t*-test. Error bars in column graphs represent standard deviation of the mean.

RNA extraction and transcriptome sequencing of A. sydowii *under PAHs biotransformation*

Fungal mycelium was harvested by centrifugation and ground in liquid nitrogen. Total RNA was isolated using the TRIzol extraction method (Thermo Fisher, Catalogue No. 15596026, USA), eluted in RNase-free water and stored at −80°C until further use. The RNA integrity was assessed on agarose gels and through capillary electrophoresis (Agilent Bioanalyzer 2100, San Diego, CA, USA). Samples were sequenced by ABM Company (Vancouver, Canada). Library construction was carried out using Illumina TruSeq mRNA library prep kit (Illumina, San Diego, CA, USA). Briefly, samples were subjected to rRNA depletion, first- and second-strand cDNA synthesis, adenylation of 3′ ends, adapter ligation, DNA fragment enrichment and real-time PCR quantification. Library quality check was performed using Qubit DNA assay and Agilent Bioanalyzer 2100. The libraries were pooled, quantified by qPCR and sequenced to 2 × 150 bp paired-end on the Illumina HiSeq-2500 platform. Transcriptome

sequencing was performed for three independent cultures/samples per group.

Transcriptome assembly and annotation

Raw reads were filtered to remove erroneous k-mers as well as adapters using Rcorrector version 1.0.4 (Song and Florea, 2015) and Trimmomatic version 0.39 (Bolger *et al*., 2014). The resulting clean reads were assembled using Trinity (Haas *et al*., 2013). BLAST software was used for functional annotation, while gene ontology (GO) annotation was performed using Blast2GO version 5.2 (Conesa *et al*., 2005). Transcript quantification was obtained using Kallisto version 0.46.1 (Bray *et al*., 2016). Raw counts were filtered out to eliminate low count transcripts (CPM < 1.5 in more than three samples) and later normalized using the RUVs method in RUVSeq version 3.2 (Risso *et al*., 2014). The transcript differential expression analysis was carried out using DESeq2 (Love *et al*., 2014). Transcripts with logFC > 1 and false discovery rate (FDR) < 0.1 were considered as differentially expressed (DE). GO enrichment analysis was performed with topGO version 3.2 (Alexa and Rahnenfuhrer, 2019) and visualized using GOplot version 1.02 (Walter *et al*., 2015). Pathway enrichment analysis was performed using BlastKOALA version 2.2 (Kanehisa *et al*., 2015).

Transcriptomic data is publicly available in National Centre for Biotechnology Information: Submission ID: SUB7393773, BioProject SRA ID: PRJNA631102.

Identification of PAH derived metabolites in culture supernatants

PAHs degradation byproducts in culture supernatant were identified using an ultra-high-performance liquid chromatography (UHPLC) Acquity I-Class System (Waters, Milford, CT, USA) with a CORTECS-UHPLC HILIC C-18 1.6 μm column (2.1 mm × 50 mm; Waters) and coupled to a Synapt G2S QToF MS (Waters). Method conditions for UHPLC and MS analysis were previously described in Mtibaà and colleagues (2018). The analysis of spectra, including *m/z* and error calculation, and metabolite identification were performed using the MassLynx *v*4.1 software (Waters, Milford, USA).

Phylogenetic and genomic analysis

The evolutionary context of the genomic potential of *Aspergillus* genus was assessed by identifying genes involved in PAH degradation in 11 *Aspergilli* and five related ascomycetous fungi where PAH biodegradation has been previously studied. Phylogenetic reconstruction was based on 33 homologous conserved protein marker sequences retrieved from genomes deposited in NCBI database. The markers used were: alaS, argS, cgtA, coaE, dnaA, gmk, ileS, infB, leuS, pgk, pheS, rnc, rplB, rplC, rplD, rplE, rplF, rplJ, rplM, rplP, rplQ, rplW, rpmA, rpsB, rpsF, rpsH, rpsI, rpsK, rpsO, secY, serS, tilS, truB (Ren *et al*., 2016). The sequences were aligned using MAFFT (Katoh and Standley, 2013), and analysed with IQ-TREE version 1.6.1 software package (Nguyen *et al*., 2015). Briefly, ModelFinder was used to determine the best-fit model for tree reconstruction (Kalyaanamoorthy *et al*., 2017). Le and Gascuel (LG) general matrix model with discrete Gamma rate heterogeneity model with four rate categories (G4 model) was chosen according to Bayesian Information Criterion (Kalyaanamoorthy *et al*., 2017). A maximum-likelihood tree was reconstructed using the IQ-TREE inference method (Nguyen *et al*., 2015). The branch supports were assessed by the ultrafast bootstrap approximation method (Minh *et al*., 2013). The obtained tree was annotated using a data matrix of gene abundance extracted from all sampled species using PFAM number to aggregate the genes corresponding to relevant enzymatic activities for PAH degradation. No scaling was applied to the data. Columns were clustered using correlation distance and average linkage using the tool Clustvis (Metsalu and Vilo, 2015).

Publicly available transcriptomic results related to PAH assimilation were analysed to produce a comprehensive comparison of DE genes involved in PAH biodegradation and detoxification, or cellular processes affected by PAHs. Transcriptional profiles from *T. verruculosus* (Gao *et al*., 2019), *A. fisheri* (Hernández-López *et al*., 2016), *A. fumigatus* (Loss *et al*., 2019) and *A. sydowii* (this study) were included in the analysis. Phylogenetic reconstruction was based on 18S rDNA genes, and ITS 1–4 and D1–D2 regions. Phylogeny was prepared according with the methodology previously mentioned in this section. *Elaphomyces morettii* was used as an outgroup. Figure 7 was prepared using iTOL version 5.0 (https://itol.embl.de) and edited in Inkscape version 1.0 (https://inkscape.org/release/inkscape-1.0/). A colour coding was used to represent upregulated (red), downregulated (blue) and non-differentially expressed genes (grey). Black was used for those genes not identified in the transcriptomic dataset.

Statistical analysis

One-way analysis of variance (ANOVA) test was conducted to determine statistically significant differences. Later, a *post hoc* multiple comparison analysis through a Tukey test was performed. Significance levels are always expressed as a value of $p < 0.05$. Data analysis software

GraphPad Prism version 7.03 (GraphPad Software) was used.

Acknowledgements

The authors are grateful to Marcela Ayala (Mexico), Nina Pastor (Mexico) and Juan E. Tacoronte (Ecuador) for their critical discussion of the metabolic pathways proposed in this work. The authors appreciate very much the attention received from Applied Biological Materials (ABM) (Vancouver, Canada) during the sequencing services. We also thank Cristian Theran Ochoa (Mexico), Kathia González (Mexico), Lyselle Ruiz de León (Mexico), Lorena Hernández-López (México), María del Rocío Rodríguez (Mexico), Olivier Savari (Canada) and Arielle Ariste (Canada) for their technical assistance. Special thanks to Prof. Jesús Mena Portales (Cuba) and Giselle Valdés Muñoz (Mexico) for helping with the figures presented in this article. Finally, authors appreciate the support of the Laboratory of Environmental Researches (Autonomous University of Morelos State, Mexico) for HPLC facilities, and the suppor received from the National Laboratory for Advanced Microscopy (CICESE). HP-G, YP-L and DG-A thank the Government of Mexico because they received a postgraduate scholarship from Conacyt. HP-G, YP-L and DG-A thank the Government of Canada for the fellowship from Emerging Leaders in Americas Program (ELAP).

Funding

This work was supported by the National Council for Science and Technology (Conacyt) of Mexico [Project Conacyt-SEP-CB-285816; Project Conacyt-DADC-311684; Project Conacyt Vocaciones Científicas 1004] and Project PRODEP-SEP-UAEMOR-PITC-381. Authors also appreciate the support from the Indo-Mexican bilateral cooperation project funded by Department of Science and Technology, Government of India along with the Conacyt, Mexico [Project Conacyt-266056 and Project DST/INT/Mexico/P-13/2016]. Also, authors appreciate the support from Conacyt through the Projects [Conacyt-SEP-CB-250831 and Conacyt-SEP-CB-252373]. No funding source influenced experimental design, writing or proofreading of the manuscript.

References

Agrawal, N., and Sushil, K.S. (2017) Degradation of polycyclic aromatic hydrocarbon (pyrene) using novel fungal strain *Coriolopsis byrsina* strain APC5. *Int Biodeter Biodegr* **122**: 69–81.

Alexa, A. and Rahnenfuhrer, J. (2019) topGO: enrichment analysis for gene ontology. R package version 2.38.1. doi: 10.18129/B9.bioc.topGO.

Ali, I., Khaliq, S., Sajid, S., and Akbar, A. (2019) Biotechnological applications of halophilic fungi: past, present, and future. In *Fungi in Extreme Environments: Ecological Role and Biotechnological Significance*, Tiquia-Arashiro, S.M., and Grube, M. (eds). Switzerland: Springer Nature, pp. 291–306.

Ali, S., Harald, G.J., Mil, v., and Richardson, M.K. (2011) Large-scale assessment of the zebrafish embryo as a possible predictive model in toxicity testing. *PLoS ONE* **6**: 1–11.

Alkio, M., Tabuchi, T.M., Wang, X., and Colón-Carmona, A. (2005) Stress responses to polycyclic aromatic hydrocarbons in arabidopsis include growth inhibition and hypersensitive response-like symptoms. *J Exp Bot* **56**: 2983–2994.

Aranda, E. (2016) Promising approaches towards biotransformation of polycyclic aromatic hydrocarbons with ascomycota fungi. *Curr Opin Biotechnol* **38**: 1–8.

Aranda, E., Godoy, P., Reina, R., Badia-Fabregat, M., Rosell, M., Marco-Urrea, E., and García-Romera, I. (2017) Isolation of ascomycota fungi with capability to transform pahs: insights into the biodegradation mechanisms of penicillium oxalicum. *Int Biodeter Biodegr* **122**: 141–150.

Batista-García, R.A., Balcázar-López, E., Miranda-Miranda, E., Sánchez-Reyes, A., Cuervo-Soto, L., Aceves-Zamudio, D., *et al*. (2014) Characterization of lignocellulolytic activities from a moderate halophile strain of *Aspergillus caesiellus* isolated from a sugarcane bagasse fermentation. *PLoS ONE* **9**: e105893.

Batista-García, R.A., Vinoth-Kumar, V., Ariste, A., Tovar-Herrera, O.E., Savary, O., Peidro-Guzmán, H., *et al*. (2017) Simple screening protocol for identification of potential mycoremediation tools for the elimination of polycyclic aromatic hydrocarbons and phenols from hyperalkalophile industrial effluents. *J Environ Manage* **198**: 1–11.

Birolli, W.G., Santos, D.A., Alvarenga, N., Garcia, A., Romão, L., and Porto, A. (2018) Biodegradation of anthracene and several pahs by the marine-derived fungus *Cladosporium* sp. CBMAI 1237. *Mar Pollut Bull* **129**: 525–533.

Bisht, S., Pandey, P., Bhargava, B., Sharma, S., Kumar, V., and Sharma, K.D. (2015) Bioremediation of polyaromatic hydrocarbons (pahs) using rhizosphere technology. *Braz J Microbiol* **46**: 7–21.

Bolger, A.M., Lohse, M., and Usadel, B. (2014) Trimmomatic: a flexible trimmer for illumina sequence data. *Bioinformatics* **30**: 2114–2120.

Bray, N.L., Pimentel, H., Melsted, P., and Pachter, L. (2016) Near-optimal probabilistic RNA-seq quantification. *Nat Biotechnol* **34**: 525–527.

Burrit, D.J. (2008) Glutathione metabolism in bryophytes under abiotic stress. In *Sulfur Assimilation and Abiotic Stress in Plants*, Khan, N.A., Singh, S., and Umar, S. (eds). Berlin, Heidelberg: Springer, pp. 111–147.

Cai, W., Li, J., and Zhang, Z. (2007) The characteristics and mechanisms of phenol biodegradation by *Fusarium* sp. *J Hazard Mater* **148**: 38–42.

Camacho-Morales, R.L., García-Fontana, C., and Fernández-Irigoyen, J. (2018) Anthracene drives subcellular proteome-wide alterations in the degradative system of *Penicillium oxalicum*. *Ecotoxicol Environ Saf* **159**: 127–135.

Chen, W., Lee, M.K., Jefcoate, C., Kim, S.C., Chen, F., and Yu, J.H. (2014) Fungal cytochrome P450 monooxygenases: their distribution, structure, functions, family

expansion, and evolutionary origin. *Genome Biol Evol* **6**: 1620–1634.

Conesa, A., Götz, S., García-Gómez, J.M., Terol, J., Talón, M., and Robles, M. (2005) Blast2GO: a universal tool for annotation, visualization and analysis in functional genomics research. *Bioinformatics* **21**: 3674–3676.

Cortis, P., Vannini, C., Cogoni, A., Mattia, F., Bracale, M., Mezzasalma, V., and Labra, M. (2016) Chemical, molecular, and proteomic analyses of moss bag biomonitoring in a petrochemical area of Sardinia (Italy). *Environ Sci Pollut Res* **23**: 2288–2300.

Daccò, C., Giromettaa, C., Asemoloye, M.D., Carpani, G., Piccoa, A.M., and Tosi, S. (2020) Key fungal degradation patterns, enzymes and their applications for the removal of aliphatic hydrocarbons in polluted soils: a review. *Int Biodeter Biodegr* **147**: 104866.

Dasari, S., Ganjayi, M.S., Yellanurkonda, P., Basha, S., and Meriga, B. (2018) Role of glutathione S-transferases in detoxification of a polycyclic aromatic hydrocarbon, methylcholanthrene. *Chem Biol Interact* **294**: 81–90.

De Vries, R.P., Riley, R., Wiebenga, A., Aguilar, G., Amillis, S., Uchima, C.A., *et al*. (2017) Comparative genomics reveals high biological diversity and specific adaptations in the industrially and medically important fungal genus *Aspergillus*. *Genome Biol* **18**: 28.

Denisov, I.G., Makris, T.M., Sligar, S.G., and Schlichting, I. (2005) Structure and chemistry of cytochrome P450. *Chem Rev* **105**: 2253–2277.

Elhusseiny, S.M., Amin, H.M., and Shebl, R.I. (2018) Modulation of laccase transcriptome during biodegradation of naphthalene by white rot fungus *Pleurotus ostreatus*. *Int Microbiol* **22**: 217–225.

El-Najjar, N., Gali-Muhtasib, H., Ketola, R.A., Vuorela, P., Urtti, A., and Vuorela, H. (2011) The chemical and biological activities of quinones: overview and implications in analytical detection. *Phytochem Rev* **10**: 353–370.

Fuchs, G., Boll, M., and Heider, J. (2011) Microbial degradation of aromatic compounds – from one strategy to four. *Nat Rev Microbiol* **9**: 803–816.

Gao, R., Hao, D.C., Hu, W., Song, S., Li, S.Y., and Ge, G.B. (2019) Transcriptome profile of polycyclic aromatic hydrocarbon-degrading fungi isolated from taxus rhizosphere. *Curr Sci* **116**: 1218–1228.

Ghosal, D., Ghosh, S., Dutta, T.K., and Ahn, Y. (2016) Current state of knowledge in microbial degradation of polycyclic aromatic hydrocarbons (PAHs): a review. *Front Microbiol* **7**: 1–27.

Gibson, D.T., and Parales, R.E. (2000) Aromatic hydrocarbon dioxygenases in environmental biotechnology. *Curr Opin Biotechnol* **11**: 236–243.

Godoy, P., Reina, R., Calderón, A., Wittich, R.M., García-Romera, I., and Aranda, E. (2016) Exploring the potential of fungi isolated from pah-polluted soil as a source of xenobiotics-degrading fungi. *Environ Sci Pollut Res* **23**: 20985–20996.

González-Abradelo, D., Pérez-Llano, Y., Peidro-Guzmán, H., Sánchez-Carbente, R., Folch-Mallol, J.L., Aranda, E., *et al*. (2019) First demonstration that ascomycetous halophilic fungi (*Aspergillus sydowii* and *Aspergillus destruens*) are useful in xenobiotic mycoremediation under high salinity conditions. *Bioresour Technol* **279**: 287–296.

Guntupalli, S., Thunuguntla, V.B.S.C., Chalasani, L.M., Rao, C.V., and Bondili, J.S. (2019) Degradation and metabolite profiling of benz (*a*) anthracene, dibenz (a, h) anthracene and indeno [1, 2, 3-cd] pyrene by *Aspergillus Terricola*. *Polycycl Aromat Compd* **39**: 84–92.

Haas, B.J., Papanicolaou, A., Yassour, M., Grabherr, M., Blood, P. D., Bowden, J., *et al*. (2013) De novo transcript sequence reconstruction from RNA-Seq using the trinity platform for reference generation and analysis. *Nat Protoc* **8**: 1494–1512.

Hadibarata, T., and Chuang, Z. (2014) Optimization of pyrene degradation by white-rot fungus *Pleurotus Pulmonarius* F043 and characterization of its metabolites. *Bioprocess Biosyst Eng* **37**: 1679–1684.

Hadibarata, T., Khudhair, A.B., Kristanti, R.A., and Kamyab, H. (2017) Biodegradation of pyrene by *Candida* Sp. S1 under high salinity conditions. *Bioprocess Biosyst Eng* **40**: 1411–1418.

Hadibarata, T., Khudhair, A.B., and Salim, M.R. (2012) Breakdown products in the metabolic pathway of anthracene degradation by a ligninolytic fungus *Polyporus* sp. S133. *Water Air Soil Pollut* **223**: 2201–2208.

Hadibarata, T., and Kristanti, R.A. (2013) Biodegradation and metabolite transformation of pyrene by basidiomycetes fungal isolate *Armillaria* Sp. F022. *Bioprocess Biosyst Eng* **36**: 461–468.

Hadibarata, T., Tachibana, S., and Askari, M. (2011) Identification of metabolites from phenanthrene oxidation by phenoloxidases and dioxygenases of *Polyporus* sp. S133. *J Microbiol Biotechnol* **21**: 299–304.

Hanschmann, E.M., Godoy, J.R., Berndt, C., Hudemann, C., and Lilling, C.H. (2013) Thioredoxins, glutaredoxins, and peroxiredoxins – molecular mechanisms and health significance: from cofactors to antioxidants to redox signaling. *Antioxid Redox Signal* **19**: 1539–1605.

Haritash, A.K., and Kaushik, C.P. (2009) Biodegradation aspects of polycyclic aromatic hydrocarbons (PAHs): a review. *J Hazard Mater* **169**: 1–15.

Harms, H., Schlosser, D., and Wick, L.Y. (2011) Untapped potential: exploiting fungi in bioremediation of hazardous chemicals. *Nat Rev Microbiol* **9**: 177–192.

Haroune, L., Saibi, S., Cabana, H., and Bellenger, J. (2016) Intracellular enzymes contribution to the biocatalytic removal of pharmaceuticals by *Trametes hirsuta*. *Environ Sci Technol* **51**: 897–904.

Herbst, F.A., Taubert, M., Jehmlich, N., Behr, T., Schmidt, F., Bergen, M., and Seifert, J. (2013) Sulfur-34s stable isotope labeling of amino acids for quantification (SULAQ34) of proteomic changes in *Pseudomonas fluorescens* during naphthalene degradation. *Mol Cell Proteomics* **12**: 2060–2069.

Hernández-López, E.L., Perezgasga, L., Huerta-Saquero, A., Mouriño-Pérez, R., and Vazquez-Duhalt, R. (2016) Biotransformation of petroleum asphaltenes and high molecular weight polycyclic aromatic hydrocarbons by *Neosartorya fischeri*. *Environ Sci Pollut Res* **23**: 10773–10784.

Hernández-López, E.L., Ramírez-Puebla, S.T., and Vazquez-Duhalt, R. (2015) Microarray nalysis of *Neosartorya fischeri* using different carbon sources, petroleum asphaltenes and glucose-peptone. *Genom Data* **5**: 235–237.

Hernández-Ortega, A., Quesne, M.G., Bui, S., Derren, J.H., Steiner, R.A., Scrutton, N.S., and Visser, S.P. (2015) Catalytic mechanism of cofactor-free dioxygenases and how they circumvent spin-forbidden oxygenation of their substrates. *J Am Chem Soc* **137**: 7474–7487.

Hickey, P.C., Swift, S.R., Roca, M.G., and Read, N.D. (2004) Live-cell imaging of filamentous fungi using vital fluorescent dyes and confocal microscopy. *Method Microbiol* **34**: 63–87.

Hidayat, A., Tachibana, S., and Itoh, K. (2012) Determination of chrysene degradation under saline conditions by Fusarium sp. F092, a fungus screened from nature. *Fungal Biology* **6**: 706–714. https://www.sciencedirect.com/science/article/pii/S1878614612000694.

Hoffmann, F., and Maser, E. (2007) Carbonyl reductases and pluripotent hydroxysteroid dehydrogenases of the short-chain dehydrogenase/reductase superfamily. *Drug Metab Rev* **39**: 87–144.

Huarte-Bonnet, C., Kumar, S., Saparrat, M.C.N., Girotti1, J. R., Santana, M., Hallsworth, J.E., and Pedrini, N. (2018) Insights into hydrocarbon assimilation by eurotialean and hypocrealean fungi: roles for CYP52 and CYP53 clans of cytochrome P450 genes. *Appl Biochem Biotechnol* **184**: 1047–1060.

Iheanacho, C.C., Okerentugba, P.O., Orji, F.A., and Ataikiru, T.L. (2014) Hydrocarbon degradation potentials of indigeneous fungal isolates from a petroleum hydrocarbon contaminated soil in Sakpenwa community. *Niger delta Jrest* **3**: 6–11.

Kadri, T., Rouissi, T., Brar, S.K., Cledon, M., Sarma,S. and Verma, M. (2016) Biodegradation of polycyclic aromatic hydrocarbons (PAHs) by fungal enzymes: a review. *J Environ Sci* **51**: 52–74.

Kalyaanamoorthy, S., Minh, B.Q., Wong, T.K.F., Haeseler, A., and Jermiin, L. (2017) ModelFinder: fast model selection for accurate phylogenetic estimates. *Nat Methods* **14**: 587–589.

Kanehisa, M., Sato, Y., and Morishima, K. (2015) BlastKOALA and ghost KOALA: KEGG tools for functional characterization of genome and metagenome sequences. *J Mol Biol* **428**: 726–731.

Kargi, F., and Dince, A.R. (2000) Use of halophilic bacteria in biological treatment of saline wastewater by fed-batch operation. *Water Environ Res* **72**: 170–174.

Katoh, K., and Standley, D.M. (2013) MAFFT multiple sequence alignment software version 7: improvements in performance and usability. *Mol Biol Evol* **30**: 772–780.

Kawale, A.S., and Povirk, L.F. (2018) Tyrosyl – DNA phosphodiesterases: rescuing the genome from the risks of relaxation. *Nucleic Acids Res* **46**: 520–537.

Kimmel, C.B., Ballard, W.W., Kimmel, S.R., Ullmann, B., and Schilling, T.F. (1995) Stages of embryonic development of the zebrafish. *Dev Dyn* **203**: 253–310.

Klose, R.J., Kallin, E.M., and Zhang, Y. (2006) JmjC-domain-containing proteins and histone demethylation. *Nat Rev Mater* **7**: 715–727.

Kristanti, R.A., and Hadibarata, T. (2015) Biodegradation and identification of transformation products of fluorene by ascomycete fungi. *Water Air Soil Pollut* **226**: 406.

Lahav, R., Fareleira, P., Nejidat, A., and Abeliovich, A. (2002) The identification and characterization of osmotolerant yeast isolates from chemical wastewater evaporation ponds. *Microb Ecol* **43**: 388–396.

Lee, H., Choi, Y.S., Kim, M.J., Huh, N.Y., Kim, G.H., Lim, Y. W., *et al*. (2010) Degrading ability of oligocyclic aromates by Phanerochaete sordida selected via screening of white rot fungi. *Folia Microbiol* **55**: 447–453.

Lee, H., Jang, Y., Choi, Y.S., Kim, M.J., Lee, J., Lee, H., *et al*. (2014) Biotechnological procedures to select white rot fungi for the degradation of PAHs. *J Microbiol Methods* **97**: 56–62.

Lenoir, I., Fontaine, J., Tisserant, B., Laruelle, F., Lounès, A., and Sahraoui, H. (2017) Beneficial contribution of the arbuscular mycorrhizal fungus, *Rhizophagus irregularis*, in the protection of *Medicago truncatula* roots against benzo [*a*] pyrene toxicity. *Mycorrhiza* **27**: 465–476.

Liu, S.H., Zeng, G.M., Niu, Q.Y., Liu, Y., Zhou, L., Jiang, L. H., *et al*. (2017) Bioremediation mechanisms of combined pollution of PAHs and heavy metals by bacteria and fungi: a mini review. *Bioresour Technol* **224**: 25–33.

Liu, Y., Bu, Q., Cao, H., Zhang, H., Liu, C., He, X., and Yun, M. (2020) Polycyclic aromatic hydrocarbons in surface water from Wuhai and Lingwu sections of the yellow river: concentrations, sources, and ecological risk. *J Chem* **2020**: 8.

Loss, E.M.O., Lee, M.K., Wu, M.Y., Martien, J., Chen, W., Amador-Noguez, D., *et al*. (2019) Cytochrome P450 monooxygenase-mediated metabolic utilization of benzo [a]pyrene by *Aspergillus* species. *Mol Biol Phys* **10**: 1–15.

Love, M.I., Huber, W., and Anders, S. (2014) Moderated estimation of fold change and dispersion for RNA-seq data with DESeq2. *Genome Biol* **15**: 550.

Maila, M.P., and Cloete, T.E. (2002) Germination of *Lepidium sativum* as a method to evaluate polycyclic aromatic hydrocarbons (PAHs) removal from contaminated soil. *Int Biodeter Biodegr* **50**: 107–113.

Manoj, K.M., and Hager, L.P. (2001) Utilization of peroxide and its relevance in oxygen insertion reactions catalyzed by chloroperoxidase. *Biochim Biophys Acta Mol Cell Res* **1547**: 408–417.

Marrs, K.A. (1996) The functions and regulation of glutathione s-transferases in plants. *Annu Rev Plant Physiol Plant Mol Biol* **47**: 127–158.

Matsui, K., Teranishi, S., Kamon, S., Kuroda, K., and Ueda, M. (2008) Discovery of a modified transcription factor endowing yeasts with organic-solvent tolerance and reconstruction of an organic-solvent-tolerant *Saccharomyces cerevisiae* strain. *Appl Environ Microbiol* **74**: 4222–4225.

Matsunaga, I., Sumimoto, T., Ayata, M., and Ogura, H. (2002) Functional modulation of a peroxygenase cytochrome P450: novel insight into the mechanisms of peroxygenase and peroxidase enzymes. *FEBS* **528**: 90–94.

McGenity, T.J. (2010) Halophilic hydrocarbon degraders. In *Handbook of Hydrocarbon and Lipid Microbiology*, Timmis, K.N. (ed). Berlin Heidelberg: Springer-Verlag, pp. 1939–1951.

Medina-Andrés, R., Solano-Peralta, A., Saucedo-Vázquez, J. P., Napsucialy-Mendivil, S., Pimentel-Cabrera, J.A., Sosa-Torres, M.E., Dubrovsky, J., and Lira-Ruan, V. (2015) The nitric oxide production in the moss physcomitrella patens is

mediated by nitrate reductase. *PLoS ONE* **10**: 1–15. https://journals.plos.org/plosone/article?id=10.1371/journal.pone.0119400.

Metsalu, T., and Vilo, J. (2015) ClustVis: a web tool for visualizing clustering of multivariate data using principal component analysis and heatmap. *Nucleic Acids Res* **43**: 566–570.

Minh, B.Q., Nguyen, M.A.T., and Haeseler, A. (2013) Ultrafast approximation for phylogenetic bootstrap. *Mol Biol Evol* **30**: 1188–1195.

Monks, T.J., and Jones, D.C. (2002) The metabolism and toxicity of quinones, quinonimines, quinone methides, and quinone-thioethers. *Curr Drug Metab* **3**: 425–438.

Morel, M., Meux, E., Mathieu, Y., Thuillier, A., Chibani, K., Harvengt, L., *et al*. (2013) Xenomic networks variability and adaptation traits in wood decaying fungi. *J Microbial Biotechnol* **6**: 248–263.

Mtibaà, R., Olicón-Hernández, D.-R., Pozo, C., Nasri, M., Mechichi, T., González, J., and Aranda, E. (2018) Degradation of bisphenol a and acute toxicity reduction by different thermo-tolerant ascomycete strains isolated from arid soils. *Ecotoxicol Environ Saf* **156**: 87–96.

Nguyen, L.T., Schmidt, H.A., Haeseler, A., and Minh, B.Q. (2015) IQ-TREE: a fast and effective stochastic algorithm for estimating maximum-likelihood phylogenies. *Mol Biol Evol* **32**: 268–274.

Ning, D., Wang, H., Ding, C., and Lu, H. (2010) Novel evidence of cytochrome P450-catalyzed oxidation of phenanthrene in *Phanerochaete chrysosporium* under ligninolytic conditions. *Biodegradation* **21**: 889–901.

Nishida, N., Ozato, N., Matsui, K., Kuroda, K., and Ueda, M. (2013) ABC transporters and cell wall proteins involved in organic solvent tolerance in *Saccharomyces cerevisiae*. *J Biotechnol* **164**: 145–152.

Nordblom, G.D., White, R.E., and Coon, M.J. (1976) Studies on hydroperoxide-dependent substrate hydroxylation by purified liver microsomal cytochrome P-450. *Arch Biochem Biophys* **175**: 524–533.

Obuekwe, C., Badrudeen, A., Al-Saleh, E., and Mulder, J. (2004) Growth and hydrocarbon degradation by three desert fungi under conditions of simultaneous temperature and salt stress. *Int Biodeter Biodegr* **56**: 197–205.

Oluwaseun, O., Oluwatoyin, B., and Angela, V. (2017) Polycyclic aromatic hydrocarbons: a critical review of environmental occurrence and bioremediation. *J Environ Manage* **60**: 758–783.

Parshikov, I.A., Woodling, K.A., and Sutherland, J.B. (2015) Biotransformations of organic compounds mediated by cultures of *Aspergillus Niger*. *Appl Microbiol Biotechnol* **99**: 6971–6986.

Passarini, M.R.Z., Sette, L.D., and Rodrigues, M.V.N. (2011) Improved extraction method to evaluate the degradation of selected PAHs by marine fungi grown in fermentative medium. *J Braz Chem Soc* **22**: 564–570.

Pernía, B., Demey, J.R., Inojosa, Y., and Naranjo-Briceño, L. (2012) Biodiversidad y potencial hidrocarbonoclastico de hongos aislados de crudo y sus derivados: Un meta-análisis. *Rev Latinoam Biotecnol Amb Algal* **3**: 1–40.

Pozdnyakova, N.N., Nikiforova, S.V., and Turkovskaya, O.V. (2010) Influence of PAHs on ligninolytic enzymes of the fungus *Pleurotus Ostreatus* D1. *Cent Eur J biol* **5**: 83–94.

Pradhan, A., Kumari, S., Dash, S., Biswal, D.P., Dash, A.K., and Panigrahi, K.C.S. (2017) Heavy metal absorption efficiency of two species of mosses (*Physcomitrella patens* and *Funaria hygrometrica*) studied in mercury treated culture under laboratory condition. *Mater Sci Eng C* **225**: 1–10.

Prenafeta, F., Hoog, G., and Summerbell, R. (2019) Fungal communities in hydrocarbon degradation. In *Microbial Communities Utilizing Hydrocarbons and Lipids: Members, Metagenomics and Ecophysiology. Handbook of Hydrocarbon and Lipid Microbiology*, McGenity, T.J. (ed). Switzerland: Springer Nature, pp. 307–342.

Qiang, L., and Cheng, J. (2019) Exposure to microplastics decreases swimming competence in larval zebrafish (*Danio rerio*). *Ecotoxicol Enviro Saf* **176**: 226–233.

Ren, R., Sun, Y., Zhao, Y., Geiser, D., Ma, H., and Zhou, X. (2016) Phylogenetic resolution of deep eukaryotic and fungal relationships using highly conserved low-copy nuclear genes. *Genome Biol Evol* **8**: 2683–2701.

Reski, R., and Abel, W.O. (1985) Induction of budding on chloronemata and caulonemata of the moss, *Physcomitrella patens*, using isopentenyladenine. *Planta* **165**: 354–358.

Risso, D., Ngai, J., Speed, T.P., and Dudoit, S. (2014) Normalization of RNA-seq data using factor analysis of control genes or samples. *Nat Biotechnol* **32**: 896–902.

Sakaki, T. (2012) Practical application of cytochrome P450. *Biol Pharm Bull* **35**: 844–849.

Singh, R., Sram, R.J., Binkova, B., Kalina, I., Popov, T.A., Georgieva, T., *et al*. (2007) The relationship between biomarkers of oxidative DNA damage, polycyclic aromatic hydrocarbon DNA adducts, antioxidant status and genetic susceptibility following exposure to environmental air pollution in humans. *Mutat Res* **620**: 83–92.

Song, L., and Florea, L. (2015) Rcorrector: efficient and accurate error correction for Illumina RNA-seq reads. *GigaScience* **4**: 1–8.

Srivastava, S., and Kumar, M. (2019) Biodegradation of polycyclic aromatic hydrocarbons (PAHs): a sustainable approach. In *Sustainable Green Technologies for Environmental Managnment*, Shah, S. (ed). Singapore: Springer Nature, pp. 111–139.

Sun, Y., Niu, W.K., Hu, X.J., Ma, X.H., Sun, Y.J., and Wen, Y. (2020) Oxidative degradation of polycyclic aromatic hydrocarbons in contaminated industrial soil using chlorine dioxide. *Chem Eng J* **394**: 124857.

Sundaramoorthy, M., Terner, J., and Poulosl, T.L. (1995) The crystal structure of chloroperoxidase: a heme peroxidase-cytochrome P450 functional hybrid. *Structure* **3**: 1367–1377.

Sutherland, J.B. and Cerniglia, C.E. (2010) Degradation of polycyclic aromatic hydrocarbons by fungi. *Handbook of Hydrocarbon and Lipid Microbiology*.

Teng, C., Wu, S., and Gong, G. (2019) Bio-removal of phenanthrene, 9-fluorenone and anthracene-9,10-dione by laccase from *Aspergillus Niger* in waste cooking oils. *Food Control* **105**: 219–225.

Thuillier, A., Chibani, K., Belli, G., Herrero, E., Dumarçay, S., Gérardin, P., *et al*. (2014) Transcriptomic responses of *Phanerochaete chrysosporium* to oak acetonic extracts: focus on a new glutathione transferase. *Appl Environ Microbiol* **80**: 6316–6327.

Thuillier, A., Ngadin, A.A., Thion, C., Billard, P., Jacquot, J. P., Gelhaye, E., and Morel, M. (2011) Functional diversification of fungal glutathione transferases from the Ure2p class. *Int J Evol Biol* **938308**: 1–9.

Tillander, V., Alexson, S.E.H., and Cohen, D.E. (2017) Deactivating fatty acids: acyl-CoA thioesterase-mediated control of lipid metabolism. *Trends Endocrinol Metab* **28**: 473–484.

Touahar, I., Haroune, L., Ba, S., Bellenger, J.P., and Cabana, JH. (2014) Characterization of combined cross-linked enzyme aggregates from laccase, versatile peroxidase and glucose oxidase, and their utilization for the elimination of pharmaceuticals. *Science of The Total Environment* **481**: 90–99. https://www.sciencedirect.com/science/article/pii/S0048969714001624.

Urlacher, V.B., and Schmid, R.D. (2004) [19] protein engineering of the cytochrome P450 monooxygenase from *Bacillus megaterium*. *Methods Enzymol* **388**: 208–224.

Vázquez-Duhalt, R., Ayala, M., and Márquez-Rocha, F.J. (2001) Biocatalytic chlorination of aromatic hydrocarbons by chloroperoxidase of *Caldariomyces fumago*. *Phytochemistry* **58**: 929–933.

Velmurugan, N., Lee, H.M., Cha, H.J., and Lee, Y.S. (2017) Proteomic analysis of the marine-derived fungus *Paecilomyces* sp. strain SF-8 in response to polycyclic aromatic hydrocarbons. *Botanica Marina* **60**: 381–392.

Verdin, A., Sahraoui, A.L.H., Newsam, R., Robinson, G., and Durand, R. (2005) Polycyclic aromatic hydrocarbons storage by *Fusarium solani* in intracellular lipid vesicles. *Environ Pollut* **133**: 283–291.

Walter, W., Sánchez-Cabo, F., and Ricote, M. (2015) GOplot: an R package for visually combining expression data with functional analysis. *Bioinformatics* **17**: 2912–2914.

Wang, C.C., Lin, Y.C., Lin, Y.C., Jhang, S.R., and Tung, C. W. (2017) Identification of informative features for predicting proinflammatory potentials of engine exhausts. *Biomed Eng Online* **16**: 1–10.

Wang, K., Huang, X., and Lin, K. (2019) Multiple catalytic roles of chloroperoxidase in the transformation of phenol: products and pathways. *Ecotoxicol Environ Saf* **179**: 96–103.

Wang, L., Li, F., Zhan, Y., and Zhu, L. (2016) Shifts in microbial community structure during in situ surfactant-enhanced bioremediation of polycyclic aromatic hydrocarbon-contaminated soil. *Environ Sci Pollut Res* **23**: 14451–14461.

Ward, O., Singh, A., and Hamme, J.V. (2003) Accelerated biodegradation of petroleum hydrocarbon waste. *J Ind Microbiol Biotechnol* **30**: 260–270.

Weisman, D., Alkio, M., and Colón-Carmona, A. (2010) Transcriptional responses to polycyclic aromatic hydrocarbon-induced stress in *Arabidopsis thaliana* reveal the involvement of hormone and defense signaling pathways. *BMC Plant Biol* **10**: 1–13.

Westerfield, M. (2000) A guide for the laboratory use of zebrafish (*Danio rerio*). *BMC Dev Biol* **203**: 169.

Winquist, E., Björklöf, K., Schultz, E., Räsänen, M., Salonen, K., Anasonye, F., *et al*. (2014) International Biodeterioration & Biodegradation Bioremediation of PAH-contaminated soil with fungi e from laboratory to fi Eld scale. *Int Biodeter Biodegr* **86**: 238–247.

Xiao, H., Smeekens, J.M., and Wu, R. (2016) Quantification of tunicamycin-induced protein expression and N-glycosylation changes in yeast. *Analyst* **141**: 3737–3745.

Yaguchi, A., Franaszek, N., O'Neill, K., Lee, S., Sitepu, I., and Boundy-Mills, K. (2020) Identification of oleaginous yeasts that metabolize aromatic compounds. *J Ind Microbiol Biotechnol* 1–13. https://doi.org/10.1007/s10295-020-02269-5.

Ye, J.S., Yin, H., Qiang, J., Peng, H., Qin, H.M., Zhang, N., and He, B.Y. (2011) Biodegradation of anthracene by *Aspergillus fumigatus*. *J Hazard Mater* **185**: 174–181.

Zafra, G., and Cortés-Espinosa, D.V. (2015) Biodegradation of polycyclic aromatic hydrocarbons by Trichoderma species: a mini review. *Environ Sci Pollut Res* **22**: 19426–19433.

Zafra, G., Moreno-Montaño, A., Absalón, A.E., and Cortés-Espinosa, D.V. (2015) Degradation of polycyclic aromatic hydrocarbons in soil by a tolerant strain of *Trichoderma asperellum*. *Environ Sci Pollut Res* **22**: 1034–1042.

Zafra, G., Taylor, T.D., Absalón, A.E., and Cortés-Espinosa, D.V. (2016) Comparative metagenomic analysis of PAH degradation in soil by a mixed microbial consortium. *J Hazard Mater* **318**: 702–710.

Zhang, J., Debets, A.J.M., Verweij, P.E., Melchers, W.J.G., Zwaan, B.J., and Schoustra, S.E. (2015) Asexual sporulation facilitates adaptation: the emergence of azole resistance in *Aspergillus fumigatus*. *Evolution* **69**: 2573–2586.

Supporting Information

Additional Supporting Information may be found in the online version of this article at the publisher's web-site:

Appendix S1: Supporting information.